Published in final edited form as:
Circ Cardiovasc Imaging. ; 16(1): . doi:10.1161/CIRCIMAGING.122.014068.

Imaging methods: magnetic resonance imaging

Katharine E. Thomas, MBBS[1,*], **Anastasia Fotaki, MD**[2,*], **Rene M. Botnar, PhD**[2,3,4], **Vanessa M. Ferreira, MD, DPhil**[1]

[1]University of Oxford Centre for Clinical Magnetic Resonance Research (OCMR), Division of Cardiovascular Medicine, Radcliffe Department of Medicine, University of Oxford, UK

[2]Department of Biomedical Engineering, School of Biomedical Engineering and Imaging Sciences, King's College London, St Thomas' Hospital, 3rd Floor-Lambeth Wing, Westminster Bridge Road, London, SE1 7EH, UK

[3]Escuela de Ingeniería, Pontificia Universidad Católica de Chile, Santiago, Chile

[4]Millennium Institute for Intelligent Healthcare Engineering, Santiago, Chile

Abstract

Myocardial inflammation occurs following activation of the cardiac immune system, producing characteristic changes in the myocardial tissue. Cardiovascular magnetic resonance (CMR) is the non-invasive imaging gold standard for myocardial tissue characterisation, and is able to detect image signal changes that may occur resulting from inflammation, including edema, hyperemia, capillary leak, necrosis, and fibrosis. Conventional CMR for the detection of myocardial inflammation and its sequela include T2-weighted imaging, parametric T1- and T2-mapping, and gadolinium-based contrast-enhanced imaging. Emerging techniques seek to image several parameters simultaneously for myocardial tissue characterisation, and to depict subtle immune-mediated changes, such as immune cell activity in the myocardium and cardiac cell metabolism. This review article outlines the underlying principles of current and emerging CMR methods for imaging myocardial inflammation.

Keywords

CMR; inflammation; immune system; parametric mapping; fingerprinting; cell labelling; hyperpolarized MRI; magnetic resonance spectroscopy; USPIO; PFC

Correspondence to: Vanessa M. Ferreira.

Correspondence to: Professor Vanessa Ferreira, University of Oxford Centre for Clinical Magnetic Resonance Research (OCMR), Level 0, John Radcliffe Hospital, Oxford OX3 9DU, vanessa.ferreira@cardiov.ox.ac.uk, Tel: +44(0)1865221172.
*joint first authors

Disclosures
None.

Europe PMC Funders Author Manuscripts

Introduction

Cardiac immune system and myocardial inflammation

The immune system in the healthy adult heart comprises all of the major leukocyte classes, including mononuclear phagocytes, neutrophils, B cells, T cells and resident macrophages [1]. In response to injury or insult, the immune system produces an inflammatory response, summarised below:

Ischemic injury/inflammation (myocardial infarction)—Insufficient oxygen delivery to myocardial tissue results in ischemia, which, if prolonged, leads to cardiomyocyte necrosis and the release of damage-associated molecular patterns. Mast cells degranulate and, along with resident macrophages and cardiomyocytes, produce inflammatory cytokines and chemokines, which lead to recruitment and production of neutrophils and monocytes. These recruited cells release further inflammatory cytokines, and further recruit immune cells. Neutrophils are cleared over the following days as the healing phase commences. Monocytes persist and differentiate into macrophages that produce growth factors, which can lead to collagen production by fibroblasts, attenuation of inflammation, and neo-angiogenesis. Within several weeks, monocyte recruitment ends and a scar forms [2,3].

Non-ischemic injury/inflammation—Non-ischemic inflammation can occur in response to a wide range of factors, such as infectious agents (including viral or bacterial), systemic immune-mediated diseases, drugs, and toxins [4]. Viral infection is the most common etiology of infectious myocarditis. A similar immune response to ischemic injury occurs, as detailed above. Additionally, where infectious agents are involved, host recognition of the antigen leads to further inflammatory cytokine production and innate immune receptor signalling, causing recruitment of natural killer (NK) cells and dendritic cells. Dendritic cells ingest dead and damaged cardiomyocytes and move to the spleen to present antigens to naïve B and T cells, which initiates activation of the adaptive immune response.

The immune response varies significantly by individual. In some, the inflammatory response is acute and comprehensive, lasting only a few weeks; in others, there is excessive or persistent activation of the immune system, with ongoing inflammation and ineffective viral clearance lasting from months to years, leading to long-term effects on the heart and its function [2,3].

The gold standard to confirm inflammation *in vivo* is through endomyocardial biopsy. This is an invasive procedure, with low diagnostic accuracy due to sampling errors, and is performed increasingly rarely [5]. However, some of the immune-mediated inflammatory changes in myocardial tissue can be detected non-invasively with cardiovascular imaging. This article will focus on cardiovascular magnetic resonance (CMR) as an imaging modality for detection of myocardial changes relating to immune-mediated inflammation.

Cardiovascular Magnetic Resonance (CMR)

CMR has become a primary tool for non-invasive assessment of various cardiovascular pathologies. In addition to structural and functional cardiac evaluation, CMR can generate contrast between different soft tissue types. This provides non-invasive myocardial tissue

characterisation, and can detect and quantify changes associated with cellular and metabolic activity in the myocardium [6].

Its principle lies in the nuclear spin, an intrinsic property of nuclei with an odd number of protons such as hydrogen, that gives rise to a small randomly oriented magnetic moment, which will produce a net magnetisation when placed within a static magnetic field (due to an excess of spins aligned with the external magnetic field). The temporal evolution of this net magnetisation, constituting of precession, excitation (nutation) and relaxation is utilised to generate MR images [7]. By employing a radio frequency pulse, the net magnetization can be tilted away from the direction of the static magnetic field thereby creating transverse magnetization that precesses at the Larmor frequency and which induces an oscillating signal in a receiver coil by Faraday induction. The transverse magnetisation (MR signal) decays at a rate given by the T2 relaxation time and the initial net magnetization is rebuilt at a rate given by the T1 relaxation time. The T1 and T2 relaxation times depend on the underlying tissue type and thus the MR signal depends on T1 and T2 as well as the choice of the pulse sequence parameters [8]. Externally administered agents may be used to enhance the visualization of variations in tissue composition, the cardiac cellular substrate and cellular metabolism.

In particular, for the visualization of myocardial inflammation, tissue alterations due to underlying edema, hyperemia, capillary leak, as well as necrosis and fibrosis (if present), can then be followed longitudinally. This can provide valuable insight into the pathogenesis of inflammatory cardiovascular disease and help determine disease severity and prognosis. MR imaging biomarkers may also be used to assess the efficacy of established or novel therapeutic interventions [9]. Established CMR methods include T1- and T2-weighted imaging, parametric (T1- and T2-) mapping, and the use of gadolinium-based contrast agents. Emerging CMR methods for assessing myocardial energetics and inflammatory cell activity can provide further insights into the pathogenesis and disease evolution of inflammatory cardiomyopathies.

Native Techniques

T2 weighted imaging

T2-weighted MR imaging represents the conventional technique for detection of myocardial edema. One widely used technique is the short-tau inversion recovery (STIR) T2-weighted sequence. It consists of two 180° pulses for the black blood preparation, followed by a third, slice-selective 180° pulse to provide the STIR contrast and null myocardial fat. The sequence utilizes segmented turbo spin echo imaging [10]. Bright-blood T2-prepared single-shot balanced steady-state free precession and hybrid TSE-SSFP sequences [11,12] are alternative T2-weighted imaging methods.

Conventional T2-weighted imaging can be analyzed in a semi-quantitative fashion by comparing the signal intensity (SI) from myocardium to a reference region of interest (ROI), either placed in relatively unaffected myocardium, or in adjacent skeletal muscle, but is subject to several artefacts and limitations [13]. These include the semi-quantitative nature of analysis, the relatively low signal-to-noise ratio (SNR) between edematous and normal

Europe PMC Funders Author Manuscripts

myocardium, signal drop-out in the lateral wall (where myocarditis tends to occur), its susceptibility to artifacts (non-suppressed blood near hypokinetic segments or the apex with slow-flowing blood), and the fact that the skeletal muscle (the reference ROI) may also be inflamed in a systemic inflammatory process, potentially resulting in false negative results.

T2-weighted imaging can depict myocardial edema in a wide range of ischemic and non-ischemic cardiac conditions, including acute myocardial infarction, myocarditis of various etiologies, Takotsubo syndrome, arrhythmogenic cardiomyopathy (ACM), cardiac transplant rejection and cardiac sarcoidosis [14]. T2-weighted-STIR can also be used to detect fluid and/or edema of the inflamed pericardium in pericarditis (Figure 1, [11]).

Parametric mapping

Newer CMR techniques that are based on quantitative pixel-wise parametric T1- and T2-mapping may circumvent many limitations of conventional CMR tissue characterisation techniques that are based on relative changes in signal intensities. Parametric mapping typically employs an exponential signal model to create quantitative pixel-by-pixel maps of the heart, without requiring normal myocardial tissue as reference within the same scan. This allows for detection of diffuse or spatially uniform disease, facilitating comparison within and between individuals over time, if the same mapping methods are employed, and scans are acquired under similar conditions [9,15].

Various MR imaging techniques (sequences) exist for both T1- and T2-mapping. Quantitative mapping methods have their own metrological properties, normal ranges, dependencies on various sequence parameters, heart rate and clinical evidence bases. The Society for Cardiovascular Magnetic Resonance (SCMR) has produced guidelines and recommendations on parametric mapping and their implementation [15]. Absolute quantitative threshold values for both T1- and T2-mapping are method-specific, with normal ranges defined as the mean plus and minus two standard deviations. Local references ranges should be established, using a minimum of 15 healthy volunteers, and benchmarked against published reported ranges. However, where small-magnitude changes are expected (such as myocardial fibrosis), high-precision reference ranges, derived from 50 or more healthy subjects, may be required [15]. The SCMR also provides guidelines and expert consensus statements on image post-processing, analysis and reporting [16]. For detection of myocardial edema, T1 or T2 values that are two standard deviations above the normal mean are generally accepted as abnormally elevated [12,15,16]. Analysis of T1 and T2 maps is currently not standardized, but may employ basic approaches (such as global or segmental values) or more advanced image analysis approaches, such as threshold-based topographic maps, textural analysis or radiomics.

Though both T1- and T2-mapping techniques can detect immune-mediated inflammation, T1 values are also extremely sensitive to tissue remodelling in the chronic setting, such as in areas of focal and diffuse fibrosis. Some studies demonstrate that T2 values can be especially sensitive to acute edema and inflammation, and less sensitive to detecting water content in fibrotic areas [17,18].

T1-mapping

T1 (spin-lattice) relaxation time is the characteristic decay constant governing the recovery of longitudinal magnetization (Mz) back to its thermal equilibrium following a radiofrequency pulse. Various T1-mapping methods exist, and can be divided broadly into two classes: (1) inversion recovery (IR)-based, such as the Modified Look-Locker Inversion recovery (MOLLI) and the Shortened Modified Look-Locker inversion recovery (ShMOLLI) methods; (2) saturation recovery (SR)-based, such as the Saturation-recovery Single-Shot Acquisition (SASHA) method. Hybrid models also exist, which use a combination of these two methods [19–22]. IR methods are the most commonly used clinically due to their larger dynamic range. Most MOLLI-based methods are sensitive to heart rate variation and arrhythmias; however, the ShMOLLI sequence is significantly less heart-rate sensitive and is able to produce excellent quality maps in patients with arrhythmia, due to a conditional reconstruction algorithm [20,23]. Saturation recovery models are heart rate independent, but generally have reduced precision and map quality compared to MOLLI-based sequences [21]. Hybrid models attempt to combine inversion recovery models and saturation recovery models, but are currently not widely used clinically. Though each sequence produces highly reproducible values when performed under similar conditions (such as the same manufacturer model of MR scanner, magnetic field strength, other hardware, software and technical parameters) [24], currently, quantitative mapping sequences are not directly comparable between MR scanners from different manufacturers, and this is an active area of development towards harmonization and standardization [15,24–27].

Native (pre-contrast) T1 values are prolonged by tissue free water content, and are typically shortened by fat and iron while post-contrast T1 values are shortened by gadolinium-based contrast agents. Increased native T1 values are seen in myocardial edema and during myocardial inflammation; this may be due to intracellular and extracellular myocardial edema, hyperemia, capillary leak, and myocyte necrosis [12]. Increased T1 values are also seen in areas of myocardial fibrosis, due to associated expansion of the extracellular space and accumulation of free water content. T1-mapping has been histologically validated via endomyocardial biopsy for the detection of myocarditis and acute myocardial inflammation and in the detection of fibrosis [12,15,18].

T1-mapping can detect chronic changes seen in various inflammatory conditions, including viral myocarditis, systemic sclerosis, rheumatoid arthritis, vasculitis, systemic lupus erythematosus and sarcoidosis [28–35]; it is also of great diagnostic value in myocardial infarction (MI), due to detection of acute myocardial edema and fibrosis/scar following the initial insult [15,36]. T1-mapping has also been histologically validated in the detection of cardiac transplant rejection, which causes necrosis and inflammation following an immune response [37].

T2-mapping

T2 (spin-spin) relaxation time is the MR constant governing the dephasing of transverse magnetization (Mx,y) after excitation. Various T2-mapping methods exist, including single-shot balanced steady-state free precession (bSSFP), gradient and spin echo (GRaSE) or fast spin echo (FSE)-based pulse sequences. Current SCMR consensus statement recommends

Europe PMC Funders Author Manuscripts

bSSFP or gradient echo pulse sequences preceded by a T2 preparation pulse, with a minimum of three T2-weighted images [15]. Most T2-mapping methods have some heart rate dependency, which can be reduced by a saturation pulse preceding the imaging sequence and T2 preparation. Similarly to T1-mapping, T2-mapping is highly reproducible when performed under similar conditions [38], but direct comparison cannot be made between scans performed with different T2-mapping sequences; harmonization and standardization of parametric mapping is an active area of development [15].

T2-mapping detects tissue free water content and is very useful for detection of acute myocardial inflammation and edema. It is superior to conventional T2-weighted imaging in diagnostic performance, and can overcome the limitations of T2-STIR, such as incomplete blood suppression, signal dropouts in the lateral wall and lower signal-to-noise ratios [39]. Due to its quantitative nature, T2-mapping can detect focal as well as global myocardial edema, without reliance on reference regions of interest and relative signal intensities.

The use of T2-mapping in the detection of myocardial inflammation has been histologically validated in humans [40]. T2-mapping can be used in the detection and monitoring myocardial inflammation in chronic systemic inflammatory diseases, such as vasculitides, systemic lupus erythematosus and sarcoidosis [30–33,41]. T2-mapping is also used in the detection of acute myocardial infarction due to the associated edema and inflammation as part of the acute immune response [42], and in the detection of acute cardiac transplantation rejection through detection of inflammation and edema following immune response [43].

T1rho

T1rho (T1ρ) measures the spin-lattice relaxation in the rotating frame, and is a sensitive marker for probing macro-molecular-water interaction [44]. T1ρ has been demonstrated to be sensitive to edema in the acute setting and scar in chronic myocardial infarction. T1ρ-mapping employs spin locking radiofrequency pulses, after nutating the thermal equilibrium net magnetization into the transverse plane using a 90° pulse. The duration and the frequency of the spin lock pulse define the T1ρ-weighting of the image. Application of T1ρ-mapping to CMR has been reported in several studies, primarily to discriminate between infarcted and healthy myocardium in animal models in a non-invasive and contrast-agent free manner [45]. Edema also induces enhancement in T1ρ MRI, as demonstrated in the area-at-risk in acutely ischemic myocardium [46]. Like T1- and T2-based MRI, the main principle for signal enhancement in T1ρ MRI appears to be edema associated increased tissue water mobility and reduction of the rotational correlation time, as demonstrated in the area-at-risk in acutely ischemic myocardium [46]. In a proof-of-principle study, patients with acute myocarditis and Takotsubo cardiomyopathy demonstrated elevated T1rho in T2-positive areas of acute myocardial injury and edema (Figure 2) [47]. This sequence is not routinely used in clinical practice, as further clinical studies are mandated for robust clinical validation.

Magnetic Resonance Fingerprinting & MR Multitasking

Cardiac Magnetic Resonance Fingerprinting (cMRF) and magnetic resonance multitasking (MRT) have recently emerged as alternative approaches to quantify rapidly and

simultaneously multiple tissue properties, including T_1, T_2, and T1rho. cMRF and MRT offer the potential to shorten and simplify scanning protocols and improve scan reproducibility. cMRF relies on highly accelerated imaging and incoherent under sampling artefacts, where acquisition parameters, such as flip angle or repetition time, vary pseudo-randomly throughout the scan to generate a unique signal evolution for every tissue, the so-called "fingerprint", defined by different combinations of T1, T2 and other parameters of interest [48]. Parametric encoding can also be increased by inserting magnetization preparation blocks (e.g., IR or T2-prep) prior to imaging. In parallel, a "dictionary" of possible signal evolutions for a sufficiently large and representative number of combinations of parameters of interest (such as T1 or T2) is generated using the specific acquisition parameters. The "fingerprint" of every voxel is then compared against all entries included in the dictionary by pattern matching (e.g. dot product or least square), to estimate the parameter combination that best represents the measured signal evolution [49].

Magnetic resonance multitasking is an alternative paradigm that can also provide multiparametric imaging. This technique captures cardiac motion, respiratory motion and relaxation parameters continuously, and can resolve the overlapping dynamics without the use of ECG triggering or breath holds. All possible signal evolutions that are taking place due to different image dynamics (i.e., T1 recovery, T2 decay, cardiac, respiratory motion) are stacked as an extra temporal dimension or "task" in a high dimensional low rank tensor (LRT), specifically designed for cardiovascular imaging [50]. cMRF and MRT are novel paradigms that can provide multiparametric tissue characterization. To-date they have been validated in healthy volunteers and in patients post myocardial infarction with good correlation to clinical reference, thus holding promise for future applications in inflammatory cardiomyopathies (Figure 3) [51,52].

Contrast-Enhanced Techniques

Gadolinium-based contrast agents

The most commonly-used MRI contrast agents exploit the paramagnetic property of the lanthanide ion, gadolinium. While the free gadolinium ion (Gd3+) itself is toxic in humans, gadolinium-based contrast agents (GBCAs) contain organic ligands that bind Gd3+ to form stable molecular complexes that can be administered intravenously and then subsequently excreted from the body. Those can be either linear or macrocyclic on the basis of the shape of the organic chelate agent, and are further subdivided as ionic or non-ionic groups. Macrocyclic GBCAs have higher structural stability than linear agents, and ionic agents tend to bind Gd3+ more tightly than non-ionic agents [53]. The biodistribution is assumed to be primarily extracellular (in intravascular and interstitial spaces). GBCAs potently shortens T1 relaxation time, and gadolinium-based contrast enhancement in-vivo is achieved by its accumulation in abnormal tissues (hence, an increase in tissue signal intensity).

Early gadolinium enhancement (EGE)—Early gadolinium enhancement (EGE) may be used as an imaging biomarker of hyperemia, capillary leakage and microcirculatory disturbance during the early vascular phase in inflammation. Image acquisition begins about 10 seconds after contrast injection (after the first pass), completing imaging during the first

3 to 5 min after injection of GBCA. For myocardial EGE, an IR-prepared fast spin echo sequence with sufficient T1-weighting is used. Pre- and post-contrast images are obtained with identical imaging parameters. Semi-quantitative comparison is made for the myocardial signal intensity enhancement relative to a skeletal muscle reference region in the same image, and then comparing pre- and post-contrast images to obtain an EGE ratio, with set cut-offs to detect significant enhancement [12]. Although EGE can provide diagnostic and prognostic information in myocarditis [54], there are several limitations, including long scan times, variable image quality and the requirement for significant expertise. EGE is one of the three original Lake Louise Criteria for using CMR to detect myocardial inflammation, but subsequent cumulative studies demonstrated that omitting EGE did not affect overall accuracy for diagnosing myocardial inflammation, despite being associated with a lower positive likelihood ratio [12]. Consequently, many centers rely on T2-based imaging and LGE for to support an imaging diagnosis of myocarditis, as per the updated Lake Louise Criteria (2018), although EGE is still used in experienced centers and in research (Figure 4 [55]) [12].

Late gadolinium enhancement (LGE)—LGE is widely used clinically for non-invasive myocardial tissue characterization. After injection of an extravascular GBCA into the bloodstream, the redistribution properties of the GBCA into the extracellular and interstitial space are exploited in LGE MRI. GBCA can persist longer in areas with extracellular space expansion, including those due to fibrosis, myocyte loss and also acute necrosis where the contrast can enter into the intracellular compartment via disrupted cell membranes [56]. This results in a relatively higher concentration of the GBCA in affected areas. By imaging following a delay of around 10 minutes after the injection and with correct nulling of normal myocardium, a higher signal in abnormal tissue is created, compared to normal, nulled myocardium. Typically, segmented inversion recovery gradient echo or bSSFP, phase-sensitive inversion-recovery (PSIR) sequences are preferred in appropriate patients with satisfactory breath-holding ability and if SNR is sufficient. Single-shot imaging (bSSFP readout) is performed as an alternative for patients with irregular heartbeat, and/or difficulty with breath holding [12]. 3D LGE and dark-blood LGE sequences are now also available [57,58]. It is emphasized that LGE reflects an expansion of extracellular space, and is not designed to detect myocardial inflammation; rather, LGE may be associated with inflammation if it leads to myocyte necrosis/fibrosis. There is a substantial body of clinical studies demonstrating that LGE provides significant diagnostic information in myocardial inflammatory diseases, including myocarditis, sarcoidosis, rheumatoid arthritis, systemic sclerosis, lupus erythematosus, peripartum cardiomyopathy and acute rejection in cardiac transplant recipients [12,59–61].

Extracellular Volume (ECV)—Myocardial inflammation, among other disease entities, may lead to extracellular space expansion. This could be due to interstitial changes in view of myocyte necrosis, focal replacement fibrosis or diffuse myocardial fibrosis (DMF) and acute extracellular edema. In the absence of other sources of ECV expansion (such as amyloidosis, edema, focal fibrosis), ECV is a surrogate marker for diffuse myocardial fibrosis [62]. ECV can be used as an adjunct to understand myocardial disease in inflammatory cardiomyopathy.

ECV estimation is based on the intravenous injection of an extracellular gadolinium-based contrast agent with non-protein-bound volume distribution; it can be measured using CMR pre- and post-contrast T1-mapping, and the hematocrit [15]. The underlying principle is that the T1 shortening effect of an extracellular GBCA on a tissue is directly related to its tissue concentration. The relationship between ECV in the myocardium and blood is approximated by this relationship, where λ is the gadolinium partition coefficient:

$$\frac{ECV_{myocardium}}{ECV_{blood}} = \lambda$$

$$\lambda = \frac{(\frac{1}{T1myo_{postGd}} - \frac{1}{T1myo_{native)}})}{(\frac{1}{T1blood_{postGd}} - \frac{1}{T1blood_{native}})}$$

$$ECV_{blood} = 1 - Hct$$

Thus, rearranging the formula and expanding the terms, the ECV of the myocardium is given as follows:

$$ECV\ myocardium = \frac{(\frac{1}{T1myo_{postGd}} - \frac{1}{T1myo_{native)}})}{(\frac{1}{T1blood_{postGd}} - \frac{1}{T1blood_{native}})} * (1 - Hct)^{15}.$$

Accurate ECV quantification is dependent upon the contrast agent having reached equilibrium within tissue compartments. Initially, quantification of myocardial ECV was achieved using the equilibrium (EQ-CMR) technique, which showed good correlation with histologic collagen volume fraction [63]. EQ-CMR assumes an equilibrium steady state between the intravascular and interstitial spaces as a strict, two-compartment model. This requires a constant infusion of contrast, and the entire procedure may last up to 2 hours. This protocol is now abbreviated by using the bolus or split-bolus contrast technique, which showed similar validation with the infusion technique [64]. The dynamic-equilibrium CMR protocol acquires a pre-contrast T1-map, followed by injection of a bolus of extravascular GBCA; after a delay of 10-15 min, a matching post-contrast T1-map is also acquired.

Confounders with regards to the accuracy of ECV estimation include incomplete dynamic equilibrium, contrast transfer into other compartments, and a faster renal clearance than exchange rate [65]. A simplified approach for the assessment of ECV is introduced where the hematocrit can be estimated from native values of blood pool T1 (“synthetic ECV”) [66,67]. The development of 3D T1-mapping acquisition are explored in 3D ECV quantification [68].

ECV has been shown to be elevated in EMB-proven acute myocarditis, correlating with edema, and in subclinical myocardial disease in rheumatoid arthritis, systemic lupus erythematosus and systemic sclerosis, likely representing low-grade inflammation and diffuse fibrosis [28,29,32].

Lake Louise Criteria for Non-Invasive Detection of Myocardial Inflammation

Due to the superior capability of CMR in the non-invasive detection of myocardial inflammation compared to other imaging modalities, the International Consensus Group on CMR Diagnosis of Myocarditis published expert consensus recommendations in 2009, known as the Lake Louise Criteria [39]. These were updated in 2018 to include parametric T1- and T2-mapping [12] (Table 1 [12,39]).

The original Lake Louise Criteria (2009) proposed that, in the setting of clinically suspected myocarditis, CMR findings are consistent with myocardial inflammation if at least “two out of three” CMR criteria were fulfilled: myocardial edema (on T2-weighted imaging), hyperemia and capillary leak (on EGE), and necrosis/fibrosis (on LGE) [39]. These had an overall diagnostic accuracy of 78% (sensitivity 67% specificity 91%) [12]. Following the development of directly quantitative pixel-wise T1- and T2-mapping, the Lake Louise criteria were updated in 2018, and revised. Probable myocardial inflammation is considered to be present on CMR if 2 out of 2 criteria were met: one positive T1-based criterion and one positive T2-based criterion (Table 1). Positive T2-based markers would be consistent with the presence of myocardial edema, an essential component of inflammation, while positive T1-based markers would be consistent more broadly with associated myocardial injury. One out of two criterion (either T1 or T2 positivity) may still support a diagnosis of myocardial inflammation, but positivity of both markers has increased specificity for an imaging diagnosis of myocardial inflammation [12]. The threshold values for positivity are method- and centre-specific, but are generally considered positive when the global or regional T1/T2 value is more than two standard deviations above the normal mean [15].

The updated Lake Louise criteria (2018) have improved diagnostic value compared to the original Lake Louise criteria (2009), with a validation cohort demonstrating an improved overall sensitivity of 88% and specificity of 96% for acute myocarditis [69]. The Lake Louise Criteria have also been shown to correlate to histopathologic findings of myocarditis [70] (Figure 5). The Lake Louise criteria have been validated mainly in patients with suspected active or acute inflammation. Compared to the acute setting, T2-mapping may be less sensitive in detecting chronic, low-grade inflammatory signal changes; while T1-mapping is highly sensitive to detecting increased free water in acute myocarditis, it is also sensitive to detection of water in more chronic settings, such as in areas affected by scarring or other causes of expanded extracellular space, and thus may not always differentiate between acute and chronic changes as a stand-alone technique [12].Nevertheless, CMR, especially with parametric mapping, has demonstrated its utility in identifying inflammation in various chronic inflammatory conditions, such as sarcoidosis, systemic sclerosis, vasculitides, systemic lupus erythematosus and rheumatoid arthritis [12]. Despite this reduced sensitivity, parametric mapping still has great utility in the identification of ongoing inflammation in chronic inflammatory conditions, such as sarcoidosis, systemic sclerosis, vasculitides, systemic lupus erythematosus and rheumatoid arthritis [28–34].

CMR Imaging of Inflammatory Cellular Activity and Myocardial Energetics

Cell labelling

Clinical CMR is currently established for non-invasive assessment of inflammation at myocardial tissue level. At the cellular level, inflammatory cells, such as macrophages/monocytes and neutrophils, play a major part in both the initiation, maintenance and resolution of inflammation. Therefore, identifying cellular activity is significant, as it can enable precise diagnosis and monitoring of disease progression, and potentially facilitate targeted therapeutic interventions. Multiple methods are under investigation, but are yet to be adopted into clinical use.

Ultrasmall superparamagnetic particles of iron oxide (USPIO)

USPIOs have been used to image macrophages in immune-mediated conditions. USPIO consist of an iron oxide core surrounded by a carbohydrate or polymer coating, and are small enough to extravasate through diseased microvessels, where they are engulfed and concentrated by tissue-resident macrophages [71]. Accumulation of USPIOs shortens T2* decay time and creates signal deficits that can be quantified and visualized using T2* MRI. Tissue properties, such as the presence of edema or hemorrhage, can modify image intensities on T2* sequences; therefore, pre- and post-contrast images need to be compared to delineate the impact of USPIO accumulation. USPIOs also have a T1 shortening effect, particularly at low concentrations, and appear bright on T1-weighted images. Rather than assessing focal image brightness at a single echo time, the T2* time constant can be calculated from the exponential decay curve using multiple echo times. This method provides greater reproducibility, broad applicability throughout the field of view, and independence from T1 effects and a range of imaging variables.

USPIO-enhanced MRI can detect tissue-resident macrophage activity and identify cellular inflammation within tissues. Preclinical and preliminary clinical studies have validated this quality in pathologies involving monocyte influx in the myocardium (autoimmune myocarditis, cardiac transplant, acute MI, Takotsubo cardiomyopathy) and plaque (atherosclerosis) [6,72–74]. Existing concerns include the difficulty to differentiate the negative contrast from potential calcification, susceptibility artifacts, and flow-related signal loss or air. Those are addressed through the recent development of off-resonance techniques that generate positive contrast, and are promising for clinical translation [75–77].

19F-enhanced CMR- perfluorocarbons

Intravenously administered perfluorocarbons (PFCs) represent an alternative approach for imaging immune cells in the cardiovascular system with CMR. PFCs are utilized as a contrast agent to visualize specific molecular targets [78] with high signal specificity, since 19F is essentially absent in living organisms. One important advantage is the creation of positive image contrast, which is directly proportional to the concentration of 19F nuclei within the tissue, providing a semi-quantitative visual assessment. Preclinical studies have utilized perfluorocarbon (PFC)-containing nanoparticles that are taken up by circulating monocytes once given intravenously. 19F hot spots due to 19F-loaded immune cells accumulation are generated at the site of inflammation in different pathologies (post

myocardial infarction, graft rejection, viral and autoimmune myocarditis) [79–82] (Figure 6, [82]). While the particular 19F containing molecule features a favorable safety profile and a biological half-life for monitoring cells over several days, its resonance spectrum is composed of several peaks, which is challenging from a MR imaging perspective. Several MR pulse sequences and reconstruction options are being explored with an aim to translate 19F-based imaging strategies into clinical practice.

Gadolinium-based activatable sensor for myeloperoxidase activity imaging

The detection of inflammation in the myocardium can also be performed by imaging a myeloperoxidase-activated gadolinium chelate (MPO-Gd). Areas with injured myocardial tissue elicit recruitment of neutrophils and monocytes, which sequentially introduce MPO. The recently developed specific MPO sensor – 5-hydroxytryptamide MPO-Gd – is activated by MPO, undergoes polymerization, binds to matrix proteins in areas of high MPO activity, and exhibits increased T1 relaxivity. This leads to increased enhancement on T1-weighted MRI [83]. Preclinical animal studies using this probe have successfully imaged oxidative stress in the myocardium, which has improved understanding of the molecular inflammatory response [83].

Magnetic resonance spectroscopy (MRS)

Current MR techniques to assess inflammation rely on the observable consequences of immune system activity via imaging signals, rather than imaging immune cell activity directly. This is due to limitations in the imaging resolution and signal-to-noise (SNR) ratio at normal temperatures and magnetic field strengths. Magnetic resonance spectroscopy (MRS), which detects individual metabolites based on their resonant frequencies, seeks to examine metabolism *in vivo*. Different nuclei and molecules can be studied using a variety of methods. Limitations include low sensitivity and technical constraints, as well as extended acquisition times [84].

Phosphorus (31-P)

Adenosine triphosphate (ATP) is the direct source of energy in the heart, and is catalysed in the mitochondria by creatine kinase to adenosine diphosphate (ADP) and phosphocreatine (PCr). PCr diffuses rapidly from the mitochondria to the myofibrils, where creatine kinase catalyzes the reformation of ATP. In the healthy heart, when ATP demand rises, ATP production will be stimulated via physiological processes. However, in the unhealthy heart (such as ischemic myocardium, or in cardiomyopathies), there is impaired energy production capacity. To maintain ATP levels, the PCr level starts to decrease and ADP levels rise. The PCr/ATP ratio will thus change. ATP, ADP and PCr can be detected via 31-Phosphorus-MRS. Each molecule creates a slightly different peak on spectroscopy, and so can be individually identified (Figure 7 [85]). We therefore can study and quantify PCr, ATP and ADP levels in hearts with inflammation [86]. A decrease in PCr to ATP ratio is seen in a range of conditions associated with myocardial inflammation, such as myocardial ischemia, heart transplant rejection, valvular heart disease, Takotsubo cardiomyopathy, and inherited cardiomyopathies [74,87–92]. In valvular heart disease and cardiomyopathies, inflammation can occur secondary to the immune response generated by pressure overload and cardiac remodelling [93]. Reduced 31-P signal and a decreased PCr:ATP ratio has also

been demonstrated in infarcted myocardial tissue in animal models [94]. Gaining real-time *in vivo* information about the myocardial energetics during inflammation is a growing and valuable area of research.

Carbon (13-C) and hyperpolarized MRI

Hyperpolarized MRI can be used to image the immune system through detection of key metabolites (such as pyruvate and fumarate) which are formed during immune cell activation due to increased metabolic requirements. Magnetic properties of external substances are manipulated to create molecular contrast agents, improving signal-to-noise (SNR) ratio by several orders of magnitude. There are different methods of hyperpolarization; however, the recent development of dissolution dynamic nuclear polarization (DNP) has significantly improved the SNR ratio to the extent that *in vivo* study of metabolic processes using 13-Carbon could be undertaken [95]. Current barriers to widespread adoption of hyperpolarized MRI are the high cost of the hyperpolarizer system, the need for extra CMR hardware that is 13-C capable, and expertise [96].

Cardiac metabolism can be studied via hyperpolarized [13-C]pyruvate. Pyruvate is an end product of glycolysis in aerobic metabolism, but also is metabolized to lactate in anaerobic metabolism. During inflammation, there is increased glycolysis following activation of immune cells and proliferation of T cells and B cells. These increased energy requirements lead to an anaerobic switch and increase in lactate production [97]. The evolving field of immunometabolic phenotyping is then able to infer inflammatory cell phenotypes and function from the metabolic changes and [13C]lactate signature seen [98,99]. Lactate production is not specific to immune cells; however, the magnitude of lactate increase in inflamed cells is such that it is easy to differentiate between these and normal tissue [99] (Figure 8).

Assessment of pyruvate metabolism *in vivo* in humans has recently been shown to be feasible [100], with early clinical studies of hyperpolarized [13C]pyruvate underway in several centers worldwide [50]. The underlying biological process driving the MR contrast in this approach is similar to the mechanism underlying high uptake of 18-FDG using PET, though hyperpolarized MR has the advantages of more rapid acquisition times, absence of ionising radiation and avoidance of the need for artificial suppression of cardiac carbohydrate metabolism.

A further hyperpolarized magnetic resonance molecule, hyperpolarized [1,4-13C2]fumarate, provides a direct MR probe of active myocardial necrosis. The fumarate-to-malate hydration reaction is catalyzed by the intracellular enzyme fumarase as part of the tricarboxylic acid cycle. Animal studies have demonstrated that myocyte necrosis exposes the [1,4-13C2] fumarate molecule to fumarase, leading to production of [1,4-13C2]malate, which does not occur when cell membranes are intact [68]. Although yet to be translated to clinical use, hyperpolarized [1,4-13C2]fumarate holds promise as a biomarker of active necrosis in inflammatory heart diseases, and could aid in detecting disease activity and evaluating response to treatment.

Sources of Funding

VMF acknowledges support from the British Heart Foundation (BHF) (CH/16/1/32013), the Oxford BHF Centre of Research Excellence, and the National Institute for Health Research (NIHR) Oxford Biomedical Research Centre at The Oxford University Hospitals NHS Foundation Trust. KET acknowledges British Heart Foundation Clinical Research Training Fellowship (FS/CRTF/21/24268).

RMB and AF acknowledge financial support from the British Heart Foundation PG/18/59/33955 and RG/20/1/34802, Engineering and Physical Sciences Research Council EP/P001009, EP/P032311/1, EP/P007619, Wellcome EPSRC (Engineering and Physical Sciences Research Council) Centre for Medical Engineering (NS/A000049/1), Millennium Institute for Intelligent Healthcare Engineering ICN2021_004 and the Department of Health via the National Institute for Health Research (NIHR) comprehensive Biomedical Research Centre award to Guy's and St. Thomas' NHS Foundation Trust.

The views expressed are those of the authors and not necessarily those of the National Health Service (NHS), the NIHR, or the Department of Health.

References

1. Litviňuková M, Talavera-López C, Maatz H, Reichart D, Worth CL, Lindberg EL, Kanda M, Polanski K, Heinig M, Lee M, et al. Cells of the adult human heart. Nature. 2020; 588: 466–472. DOI: 10.1038/s41586-020-2797-4 [PubMed: 32971526]
2. Swirski FK, Nahrendorf M. Cardioimmunology: the immune system in cardiac homeostasis and disease. Nature Reviews Immunology. 2018; 18: 733–744. DOI: 10.1038/s41577-018-0065-8
3. Tschöpe C, Ammirati E, Bozkurt B, Caforio ALP, Cooper LT, Felix SB, Hare JM, Heidecker B, Heymans S, Hübner N, et al. Myocarditis and inflammatory cardiomyopathy: current evidence and future directions. Nature Reviews Cardiology. 2021; 18: 169–193. DOI: 10.1038/s41569-020-00435-x [PubMed: 33046850]
4. Caforio AL, Pankuweit S, Arbustini E, Basso C, Gimeno-Blanes J, Felix SB, Fu M, Heliö T, Heymans S, Jahns R, et al. Current state of knowledge on aetiology, diagnosis, management, and therapy of myocarditis: a position statement of the European Society of Cardiology Working Group on Myocardial and Pericardial Diseases. Eur Heart J. 2013; 34: 2636–2648. 2648a-2648d doi: 10.1093/eurheartj/eht210 [PubMed: 23824828]
5. Cooper LT, Baughman KL, Feldman AM, Frustaci A, Jessup M, Kuhl U, Levine GN, Narula J, Starling RC, Towbin J, et al. The Role of Endomyocardial Biopsy in the Management of Cardiovascular Disease. Circulation. 2007; 116: 2216–2233. DOI: 10.1161/CIRCULATIONAHA.107.186093 [PubMed: 17959655]
6. Stirrat CG, Alam SR, MacGillivray TJ, Gray CD, Dweck MR, Raftis J, Jenkins WS, Wallace WA, Pessotto R, Lim KH, et al. Ferumoxytol-enhanced magnetic resonance imaging assessing inflammation after myocardial infarction. Heart. 2017; 103: 1528–1535. DOI: 10.1136/heartjnl-2016-311018 [PubMed: 28642288]
7. Vassiliou VS, Cameron D, Prasad SK, Gatehouse PD. Magnetic resonance imaging: Physics basics for the cardiologist. JRSM Cardiovasc Dis. 2018; 7 2048004018772237 doi: 10.1177/2048004018772237 [PubMed: 30128147]
8. Ridgway JP. Cardiovascular magnetic resonance physics for clinicians: part I. Journal of Cardiovascular Magnetic Resonance. 2010; 12: 71. doi: 10.1186/1532-429X-12-71 [PubMed: 21118531]
9. Polte CL, Bobbio E, Bollano E, Bergh N, Polte C, Himmelman J, Lagerstrand KM, Gao SA. Cardiovascular Magnetic Resonance in Myocarditis. Diagnostics (Basel). 2022; 12: 399. doi: 10.3390/diagnostics12020399 [PubMed: 35204490]
10. Biglands JD, Radjenovic A, Ridgway JP. Cardiovascular magnetic resonance physics for clinicians: part II. Journal of Cardiovascular Magnetic Resonance. 2012; 14: 66. doi: 10.1186/1532-429X-14-66 [PubMed: 22995744]
11. Friedrich MG, Marcotte F. Cardiac Magnetic Resonance Assessment of Myocarditis. Circulation: Cardiovascular Imaging. 2013; 6: 833–839. DOI: 10.1161/CIRCIMAGING.113.000416 [PubMed: 24046380]

12. Ferreira VM, Schulz-Menger J, Holmvang G, Kramer CM, Carbone I, Sechtem U, Kindermann I, Gutberlet M, Cooper LT, Liu P, et al. Cardiovascular Magnetic Resonance in Nonischemic Myocardial Inflammation: Expert Recommendations. J Am Coll Cardiol. 2018; 72: 3158–3176. DOI: 10.1016/j.jacc.2018.09.072 [PubMed: 30545455]

13. Abdel-Aty H, Boyé P, Zagrosek A, Wassmuth R, Kumar A, Messroghli D, Bock P, Dietz R, Friedrich Matthias G, Schulz-Menger J. Diagnostic Performance of Cardiovascular Magnetic Resonance in Patients With Suspected Acute Myocarditis. Journal of the American College of Cardiology. 2005; 45: 1815–1822. DOI: 10.1016/j.jacc.2004.11.069 [PubMed: 15936612]

14. Eitel I, Friedrich MG. T2-weighted cardiovascular magnetic resonance in acute cardiac disease. Journal of Cardiovascular Magnetic Resonance. 2011; 13: 13. doi: 10.1186/1532-429X-13-13 [PubMed: 21332972]

15. Messroghli DR, Moon JC, Ferreira VM, Grosse-Wortmann L, He T, Kellman P, Mascherbauer J, Nezafat R, Salerno M, Schelbert EB, et al. Clinical recommendations for cardiovascular magnetic resonance mapping of T1, T2, T2* and extracellular volume: A consensus statement by the Society for Cardiovascular Magnetic Resonance (SCMR) endorsed by the European Association for Cardiovascular Imaging (EACVI). J Cardiovasc Magn Reson. 2017; 19: 75. doi: 10.1186/s12968-017-0389-8 [PubMed: 28992817]

16. Schulz-Menger J, Bluemke DA, Bremerich J, Flamm SD, Fogel MA, Friedrich MG, Kim RJ, von Knobelsdorff-Brenkenhoff F, Kramer CM, Pennell DJ, et al. Standardized image interpretation and post-processing in cardiovascular magnetic resonance - 2020 update. Journal of Cardiovascular Magnetic Resonance. 2020; 22: 19. doi: 10.1186/s12968-020-00610-6 [PubMed: 32160925]

17. von Knobelsdorff-Brenkenhoff F, Schüler J, Dogangüzel S, Dieringer MA, Rudolph A, Greiser A, Kellman P, Schulz-Menger J. Detection and Monitoring of Acute Myocarditis Applying Quantitative Cardiovascular Magnetic Resonance. Circ Cardiovasc Imaging. 2017; 10 e005242 doi: 10.1161/circimaging.116.005242 [PubMed: 28213448]

18. Kotanidis CP, Bazmpani MA, Haidich AB, Karvounis C, Antoniades C, Karamitsos TD. Diagnostic Accuracy of Cardiovascular Magnetic Resonance in Acute Myocarditis: A Systematic Review and Meta-Analysis. JACC Cardiovasc Imaging. 2018; 11: 1583–1590. DOI: 10.1016/j.jcmg.2017.12.008 [PubMed: 29454761]

19. Messroghli DR, Radjenovic A, Kozerke S, Higgins DM, Sivananthan MU, Ridgway JP. Modified Look-Locker inversion recovery (MOLLI) for high-resolution T1 mapping of the heart. Magn Reson Med. 2004; 52: 141–146. DOI: 10.1002/mrm.20110 [PubMed: 15236377]

20. Piechnik SK, Ferreira VM, Dall'Armellina E, Cochlin LE, Greiser A, Neubauer S, Robson MD. Shortened Modified Look-Locker Inversion recovery (ShMOLLI) for clinical myocardial T1-mapping at 1.5 and 3 T within a 9 heartbeat breathhold. J Cardiovasc Magn Reson. 2010; 12: 69. doi: 10.1186/1532-429x-12-69 [PubMed: 21092095]

21. Chow K, Flewitt JA, Green JD, Pagano JJ, Friedrich MG, Thompson RB. Saturation recovery single-shot acquisition (SASHA) for myocardial T(1) mapping. Magn Reson Med. 2014; 71: 2082–2095. DOI: 10.1002/mrm.24878 [PubMed: 23881866]

22. Weingärtner S, Akçakaya M, Basha T, Kissinger KV, Goddu B, Berg S, Manning WJ, Nezafat R. Combined saturation/inversion recovery sequences for improved evaluation of scar and diffuse fibrosis in patients with arrhythmia or heart rate variability. Magn Reson Med. 2014; 71: 1024–1034. DOI: 10.1002/mrm.24761 [PubMed: 23650078]

23. Ferreira VM, Wijesurendra RS, Liu A, Greiser A, Casadei B, Robson MD, Neubauer S, Piechnik SK. Systolic ShMOLLI myocardial T1-mapping for improved robustness to partial-volume effects and applications in tachyarrhythmias. Journal of Cardiovascular Magnetic Resonance. 2015; 17: 77. doi: 10.1186/s12968-015-0182-5 [PubMed: 26315682]

24. Piechnik SK, Ferreira VM, Lewandowski AJ, Ntusi NAB, Banerjee R, Holloway C, Hofman MBM, Sado DM, Maestrini V, White SK, et al. Normal variation of magnetic resonance T1 relaxation times in the human population at 1.5 T using ShMOLLI. Journal of Cardiovascular Magnetic Resonance. 2013; 15: 13. doi: 10.1186/1532-429X-15-13 [PubMed: 23331520]

25. Dabir D, Child N, Kalra A, Rogers T, Gebker R, Jabbour A, Plein S, Yu C-Y, Otton J, Kidambi A, et al. Reference values for healthy human myocardium using a T1 mapping methodology: results from the International T1 Multicenter cardiovascular magnetic resonance study. Journal

of Cardiovascular Magnetic Resonance. 2014; 16: 69. doi: 10.1186/s12968-014-0069-x [PubMed: 25384607]

26. Popescu IA, Werys K, Zhang Q, Puchta H, Hann E, Lukaschuk E, Ferreira VM, Piechnik SK. Standardization of T1-mapping in cardiovascular magnetic resonance using clustered structuring for benchmarking normal ranges. International Journal of Cardiology. 2021; 326: 220–225. DOI: 10.1016/j.ijcard.2020.10.041 [PubMed: 33096146]
27. Zhang Q, Werys K, Popescu IA, Biasiolli L, Ntusi NAB, Desai M, Zimmerman SL, Shah DJ, Autry K, Kim B, et al. Quality assurance of quantitative cardiac T1-mapping in multicenter clinical trials – A T1 phantom program from the hypertrophic cardiomyopathy registry (HCMR) study. International Journal of Cardiology. 2021; 330: 251–258. DOI: 10.1016/j.ijcard.2021.01.026 [PubMed: 33535074]
28. Ntusi NA, Piechnik SK, Francis JM, Ferreira VM, Rai A, Matthews PM, Robson MD, Moon J, Wordsworth PB, Neubauer S. Subclinical myocardial inflammation and diffuse fibrosis are common in systemic sclerosis–a clinical study using myocardial T1-mapping and extracellular volume quantification. Journal of Cardiovascular Magnetic Resonance. 2014; 16: 1–12. [PubMed: 24387349]
29. Ntusi NAB, Piechnik SK, Francis JM, Ferreira VM, Matthews PM, Robson MD, Wordsworth PB, Neubauer S, Karamitsos TD. Diffuse Myocardial Fibrosis and Inflammation in Rheumatoid Arthritis: Insights From CMR T1 Mapping. JACC Cardiovasc Imaging. 2015; 8: 526–536. DOI: 10.1016/j.jcmg.2014.12.025 [PubMed: 25890584]
30. Greulich S, Mayr A, Kitterer D, Latus J, Henes J, Steubing H, Kaesemann P, Patrascu A, Greiser A, Groeninger S, et al. T1 and T2 mapping for evaluation of myocardial involvement in patients with ANCA-associated vasculitides. J Cardiovasc Magn Reson. 2017; 19: 6. doi: 10.1186/s12968-016-0315-5 [PubMed: 28077133]
31. Mayr A, Kitterer D, Latus J, Steubing H, Henes J, Vecchio F, Kaesemann P, Patrascu A, Greiser A, Groeninger S, et al. Evaluation of myocardial involvement in patients with connective tissue disorders: a multi-parametric cardiovascular magnetic resonance study. J Cardiovasc Magn Reson. 2016; 18: 67. doi: 10.1186/s12968-016-0288-4 [PubMed: 27733210]
32. Puntmann VO, D'Cruz D, Smith Z, Pastor A, Choong P, Voigt T, Carr-White G, Sangle S, Schaeffter T, Nagel E. Native myocardial T1 mapping by cardiovascular magnetic resonance imaging in subclinical cardiomyopathy in patients with systemic lupus erythematosus. Circ Cardiovasc Imaging. 2013; 6: 295–301. DOI: 10.1161/circimaging.112.000151 [PubMed: 23403334]
33. Puntmann VO, Isted A, Hinojar R, Foote L, Carr-White G, Nagel E. T1 and T2 Mapping in Recognition of Early Cardiac Involvement in Systemic Sarcoidosis. Radiology. 2017; 285: 63–72. DOI: 10.1148/radiol.2017162732 [PubMed: 28448233]
34. Ntusi NAB, Francis JM, Sever E, Liu A, Piechnik SK, Ferreira VM, Matthews PM, Robson MD, Wordsworth PB, Neubauer S, et al. Anti-TNF modulation reduces myocardial inflammation and improves cardiovascular function in systemic rheumatic diseases. Int J Cardiol. 2018; 270: 253–259. DOI: 10.1016/j.ijcard.2018.06.099 [PubMed: 30017519]
35. Ferreira VM, Piechnik SK, Dall'Armellina E, Karamitsos TD, Francis JM, Ntusi N, Holloway C, Choudhury RP, Kardos A, Robson MD, et al. T(1) mapping for the diagnosis of acute myocarditis using CMR: comparison to T2-weighted and late gadolinium enhanced imaging. JACC Cardiovasc Imaging. 2013; 6: 1048–1058. DOI: 10.1016/j.jcmg.2013.03.008 [PubMed: 24011774]
36. Dastidar AG, Harries I, Pontecorboli G, Bruno VD, De Garate E, Moret C, Baritussio A, Johnson TW, McAlindon E, Bucciarelli-Ducci C. Native T1 mapping to detect extent of acute and chronic myocardial infarction: comparison with late gadolinium enhancement technique. Int J Cardiovasc Imaging. 2019; 35: 517–527. DOI: 10.1007/s10554-018-1467-1 [PubMed: 30357547]
37. Imran M, Wang L, McCrohon J, Yu C, Holloway C, Otton J, Huang J, Stehning C, Moffat KJ, Ross J, et al. Native T(1) Mapping in the Diagnosis of Cardiac Allograft Rejection: A Prospective Histologically Validated Study. JACC Cardiovasc Imaging. 2019; 12: 1618–1628. DOI: 10.1016/j.jcmg.2018.10.027 [PubMed: 30660547]
38. Wiesmueller M, Wuest W, Heiss R, Treutlein C, Uder M, May MS. Cardiac T2 mapping: robustness and homogeneity of standardized in-line analysis. Journal of Cardiovascular Magnetic Resonance. 2020; 22: 39. doi: 10.1186/s12968-020-00619-x [PubMed: 32460852]

39. Friedrich MG, Sechtem U, Schulz-Menger J, Holmvang G, Alakija P, Cooper LT, White JA, Abdel-Aty H, Gutberlet M, Prasad S, et al. Cardiovascular magnetic resonance in myocarditis: A JACC White Paper. Journal of the American College of Cardiology. 2009; 53: 1475–1487. DOI: 10.1016/j.jacc.2009.02.007 [PubMed: 19389557]
40. Bohnen S, Radunski UK, Lund GK, Kandolf R, Stehning C, Schnackenburg B, Adam G, Blankenberg S, Muellerleile K. Performance of t1 and t2 mapping cardiovascular magnetic resonance to detect active myocarditis in patients with recent-onset heart failure. Circ Cardiovasc Imaging. 2015; 8 e003073 doi: 10.1161/circimaging.114.003073 [PubMed: 26015267]
41. Zhang Y, Corona-Villalobos CP, Kiani AN, Eng J, Kamel IR, Zimmerman SL, Petri M. Myocardial T2 mapping by cardiovascular magnetic resonance reveals subclinical myocardial inflammation in patients with systemic lupus erythematosus. Int J Cardiovasc Imaging. 2015; 31: 389–397. DOI: 10.1007/s10554-014-0560-3 [PubMed: 25352245]
42. Giri S, Chung YC, Merchant A, Mihai G, Rajagopalan S, Raman SV, Simonetti OP. T2 quantification for improved detection of myocardial edema. J Cardiovasc Magn Reson. 2009; 11: 56. doi: 10.1186/1532-429x-11-56 [PubMed: 20042111]
43. Vermes E, Pantaléon C, Auvet A, Cazeneuve N, Machet MC, Delhommais A, Bourguignon T, Aupart M, Brunereau L. Cardiovascular magnetic resonance in heart transplant patients: diagnostic value of quantitative tissue markers: T2 mapping and extracellular volume fraction, for acute rejection diagnosis. J Cardiovasc Magn Reson. 2018; 20: 59. doi: 10.1186/s12968-018-0480-9 [PubMed: 30153847]
44. Muthupillai R, Flamm SD, Wilson JM, Pettigrew RI, Dixon WT. Acute myocardial infarction: tissue characterization with T1ρ-weighted MR imaging—initial experience. Radiology. 2004; 232: 606–610. [PubMed: 15215547]
45. Musthafa HS, Dragneva G, Lottonen L, Merentie M, Petrov L, Heikura T, Ylä-Herttuala E, Ylä-Herttuala S, Gröhn O, Liimatainen T. Longitudinal rotating frame relaxation time measurements in infarcted mouse myocardium in vivo. Magn Reson Med. 2013; 69: 1389–1395. DOI: 10.1002/mrm.24382 [PubMed: 22736543]
46. Han Y, Liimatainen T, Gorman RC, Witschey WR. Assessing Myocardial Disease Using T(1ρ) MRI. Curr Cardiovasc Imaging Rep. 2014; 7 9248 doi: 10.1007/s12410-013-9248-7 [PubMed: 24688628]
47. Bustin A, Toupin S, Sridi S, Yerly J, Bernus O, Labrousse L, Quesson B, Rogier J, Haïssaguerre M, van Heeswijk R, et al. Endogenous assessment of myocardial injury with single-shot model-based non-rigid motion-corrected T1 rho mapping. J Cardiovasc Magn Reson. 2021; 23: 119. doi: 10.1186/s12968-021-00781-w [PubMed: 34670572]
48. Ma D, Gulani V, Seiberlich N, Liu K, Sunshine JL, Duerk JL, Griswold MA. Magnetic resonance fingerprinting. Nature. 2013; 495: 187–192. DOI: 10.1038/nature11971 [PubMed: 23486058]
49. Velasco C, Cruz G, Jaubert O, Lavin B, Botnar RM, Prieto C. Simultaneous comprehensive liver T1, T2, T 2 *, T1rho, and fat fraction characterization with MR fingerprinting. Magn Reson Med. 2022; 87: 1980–1991. DOI: 10.1002/mrm.29089 [PubMed: 34792212]
50. Christodoulou AG, Shaw JL, Nguyen C, Yang Q, Xie Y, Wang N, Li D. Magnetic resonance multitasking for motion-resolved quantitative cardiovascular imaging. Nat Biomed Eng. 2018; 2: 215–226. DOI: 10.1038/s41551-018-0217-y [PubMed: 30237910]
51. Velasco C, Cruz G, Lavin B, Hua A, Fotaki A, Botnar RM, Prieto C. Simultaneous T1, T2, and T1rho cardiac magnetic resonance fingerprinting for contrast agent-free myocardial tissue characterization. Magn Reson Med. 2022; 87: 1992–2002. DOI: 10.1002/mrm.29091 [PubMed: 34799854]
52. Jaubert O, Cruz G, Bustin A, Hajhosseiny R, Nazir S, Schneider T, Koken P, Doneva M, Rueckert D, Masci PG, et al. T1, T2, and Fat Fraction Cardiac MR Fingerprinting: Preliminary Clinical Evaluation. J Magn Reson Imaging. 2021; 53: 1253–1265. DOI: 10.1002/jmri.27415 [PubMed: 33124081]
53. Fraum TJ, Ludwig DR, Bashir MR, Fowler KJ. Gadolinium-based contrast agents: A comprehensive risk assessment. J Magn Reson Imaging. 2017; 46: 338–353. DOI: 10.1002/jmri.25625 [PubMed: 28083913]
54. Yuan W-F, Zhao X-X, Hu F-B, Bai C, Tang F. Evaluation of Early Gadolinium Enhancement (EGE) and Cardiac Functional Parameters in Cine-Magnetic Resonance Imaging (MRI) on

Artificial Intelligence in Patients with Acute Myocarditis: A Case-Controlled Observational Study. Med Sci Monit. 2019; 25: 5493–5500. DOI: 10.12659/MSM.916690 [PubMed: 31378779]

55. Lombardi, M, Plein, S, Petersen, S, Bucciarelli-Ducci, C, Valsangiacomo Buechel, E, Basso, C, Ferrari, V. The EACVI Textbook of Cardiovascular Magnetic Resonance. Oxford, UK: Oxford University Press; 2018.
56. Haaf P, Garg P, Messroghli DR, Broadbent DA, Greenwood JP, Plein S. Cardiac T1 Mapping and Extracellular Volume (ECV) in clinical practice: a comprehensive review. J Cardiovasc Magn Reson. 2016; 18: 89. doi: 10.1186/s12968-016-0308-4 [PubMed: 27899132]
57. Basha TA, Akçakaya M, Liew C, Tsao CW, Delling FN, Addae G, Ngo L, Manning WJ, Nezafat R. Clinical performance of high-resolution late gadolinium enhancement imaging with compressed sensing. J Magn Reson Imaging. 2017; 46: 1829–1838. DOI: 10.1002/jmri.25695 [PubMed: 28301075]
58. Holtackers RJ, Van De Heyning CM, Nazir MS, Rashid I, Ntalas I, Rahman H, Botnar RM, Chiribiri A. Clinical value of dark-blood late gadolinium enhancement cardiovascular magnetic resonance without additional magnetization preparation. J Cardiovasc Magn Reson. 2019; 21: 44. doi: 10.1186/s12968-019-0556-1 [PubMed: 31352900]
59. Bière L, Piriou N, Ernande L, Rouzet F, Lairez O. Imaging of myocarditis and inflammatory cardiomyopathies. Archives of Cardiovascular Diseases. 2019; 112: 630–641. DOI: 10.1016/j.acvd.2019.05.007 [PubMed: 31494082]
60. Grani C, Eichhorn C, Biere L, Murthy VL, Agarwal V, Kaneko K, Cuddy S, Aghayev A, Steigner M, Blankstein R. Prognostic value of cardiac magnetic resonance tissue characterization in risk stratifying patients with suspected myocarditis. Journal of the American College of Cardiology. 2017; 70: 1964–1976. [PubMed: 29025553]
61. Marie PY, Angioï M, Carteaux JP, Escanye JM, Mattei S, Tzvetanov K, Claudon O, Hassan N, Danchin N, Karcher G, et al. Detection and prediction of acute heart transplant rejection with the myocardial T2 determination provided by a black-blood magnetic resonance imaging sequence. J Am Coll Cardiol. 2001; 37: 825–831. DOI: 10.1016/s0735-1097(00)01196-7 [PubMed: 11693758]
62. Moon JC, Messroghli DR, Kellman P, Piechnik SK, Robson MD, Ugander M, Gatehouse PD, Arai AE, Friedrich MG, Neubauer S, et al. Myocardial T1 mapping and extracellular volume quantification: a Society for Cardiovascular Magnetic Resonance (SCMR) and CMR Working Group of the European Society of Cardiology consensus statement. J Cardiovasc Magn Reson. 2013; 15: 92. doi: 10.1186/1532-429X-15-92 [PubMed: 24124732]
63. Flett AS, Hayward MP, Ashworth MT, Hansen MS, Taylor AM, Elliott PM, McGregor C, Moon JC. Equilibrium Contrast Cardiovascular Magnetic Resonance for the Measurement of Diffuse Myocardial Fibrosis. Circulation. 2010; 122: 138–144. DOI: 10.1161/CIRCULATIONAHA.109.930636 [PubMed: 20585010]
64. White SK, Sado DM, Fontana M, Banypersad SM, Maestrini V, Flett AS, Piechnik SK, Robson MD, Hausenloy DJ, Sheikh AM, et al. T1 Mapping for Myocardial Extracellular Volume Measurement by CMR: Bolus Only Versus Primed Infusion Technique. JACC: Cardiovascular Imaging. 2013; 6: 955–962. DOI: 10.1016/j.jcmg.2013.01.011 [PubMed: 23582361]
65. Miller CA, Naish JH, Bishop P, Coutts G, Clark D, Zhao S, Ray SG, Yonan N, Williams SG, Flett AS, et al. Comprehensive Validation of Cardiovascular Magnetic Resonance Techniques for the Assessment of Myocardial Extracellular Volume. Circulation: Cardiovascular Imaging. 2013; 6: 373–383. DOI: 10.1161/CIRCIMAGING.112.000192 [PubMed: 23553570]
66. Treibel TA, Fontana M, Maestrini V, Castelletti S, Rosmini S, Simpson J, Nasis A, Bhuva AN, Bulluck H, Abdel-Gadir A, et al. Automatic Measurement of the Myocardial Interstitium. JACC: Cardiovascular Imaging. 2016; 9: 54–63. DOI: 10.1016/j.jcmg.2015.11.008 [PubMed: 26762875]
67. Chen W, Doeblin P, Al-Tabatabaee S, Klingel K, Tanacli R, Jakob Weiß K, Stehning C, Patel AR, Pieske B, Zou J, et al. Synthetic Extracellular Volume in Cardiac Magnetic Resonance Without Blood Sampling: a Reliable Tool to Replace Conventional Extracellular Volume. Circ Cardiovasc Imaging. 2022; 15 e013745 doi: 10.1161/circimaging.121.013745 [PubMed: 35360924]
68. Robinson AA, Chow K, Salerno M. Myocardial T1 and ECV Measurement: Underlying Concepts and Technical Considerations. JACC Cardiovasc Imaging. 2019; 12: 2332–2344. DOI: 10.1016/j.jcmg.2019.06.031 [PubMed: 31542529]

69. Luetkens JA, Faron A, Isaak A, Dabir D, Kuetting D, Feisst A, Schmeel FC, Sprinkart AM, Thomas D. Comparison of Original and 2018 Lake Louise Criteria for Diagnosis of Acute Myocarditis: Results of a Validation Cohort. Radiology: Cardiothoracic Imaging. 2019; 1 e190010 doi: 10.1148/ryct.2019190010 [PubMed: 33778510]

70. Li S, Duan X, Feng G, Sirajuddin A, Yin G, Zhuang B, He J, Xu J, Yang W, Wu W, et al. Multiparametric Cardiovascular Magnetic Resonance in Acute Myocarditis: Comparison of 2009 and 2018 Lake Louise Criteria With Endomyocardial Biopsy Confirmation. Front Cardiovasc Med. 2021; 8 739892 doi: 10.3389/fcvm.2021.739892 [PubMed: 34712710]

71. Ruehm SG, Corot C, Vogt P, Kolb S, Debatin JF. Magnetic resonance imaging of atherosclerotic plaque with ultrasmall superparamagnetic particles of iron oxide in hyperlipidemic rabbits. Circulation. 2001; 103: 415–422. DOI: 10.1161/01.cir.103.3.415 [PubMed: 11157694]

72. Morris JB, Olzinski AR, Bernard RE, Aravindhan K, Mirabile RC, Boyce R, Willette RN, Jucker BM. p38 MAPK inhibition reduces aortic ultrasmall superparamagnetic iron oxide uptake in a mouse model of atherosclerosis: MRI assessment. Arterioscler Thromb Vasc Biol. 2008; 28: 265–271. DOI: 10.1161/atvbaha.107.151175 [PubMed: 18162612]

73. Kanno S, Wu YJ, Lee PC, Dodd SJ, Williams M, Griffith BP, Ho C. Macrophage accumulation associated with rat cardiac allograft rejection detected by magnetic resonance imaging with ultrasmall superparamagnetic iron oxide particles. Circulation. 2001; 104: 934–938. DOI: 10.1161/hc3401.093148 [PubMed: 11514382]

74. Tsampasian V, Swift AJ, Assadi H, Chowdhary A, Swoboda P, Sammut E, Dastidar A, Cabrero JB, Del Val JR, Nair S, et al. Myocardial inflammation and energetics by cardiac MRI: a review of emerging techniques. BMC Med Imaging. 2021; 21: 164. doi: 10.1186/s12880-021-00695-0 [PubMed: 34749671]

75. Stuber M, Gilson WD, Schär M, Kedziorek DA, Hofmann LV, Shah S, Vonken EJ, Bulte JW, Kraitchman DL. Positive contrast visualization of iron oxide-labeled stem cells using inversion-recovery with ON-resonant water suppression (IRON). Magn Reson Med. 2007; 58: 1072–1077. DOI: 10.1002/mrm.21399 [PubMed: 17969120]

76. Farrar CT, Dai G, Novikov M, Rosenzweig A, Weissleder R, Rosen BR, Sosnovik DE. Impact of field strength and iron oxide nanoparticle concentration on the linearity and diagnostic accuracy of off-resonance imaging. NMR Biomed. 2008; 21: 453–463. DOI: 10.1002/nbm.1209 [PubMed: 17918777]

77. Mani V, Briley-Saebo KC, Itskovich VV, Samber DD, Fayad ZA. Gradient echo acquisition for superparamagnetic particles with positive contrast (GRASP): sequence characterization in membrane and glass superparamagnetic iron oxide phantoms at 1.5T and 3T. Magn Reson Med. 2006; 55: 126–135. DOI: 10.1002/mrm.20739 [PubMed: 16342148]

78. Temme S, Grapentin C, Quast C, Jacoby C, Grandoch M, Ding Z, Owenier C, Mayenfels F, Fischer JW, Schubert R, et al. Noninvasive Imaging of Early Venous Thrombosis by 19F Magnetic Resonance Imaging With Targeted Perfluorocarbon Nanoemulsions. Circulation. 2015; 131: 1405–1414. DOI: 10.1161/circulationaha.114.010962 [PubMed: 25700177]

79. Bönner F, Jacoby C, Temme S, Borg N, Ding Z, Schrader J, Flögel U. Multifunctional MR monitoring of the healing process after myocardial infarction. Basic research in cardiology. 2014; 109: 1–15.

80. Flögel U, Su S, Kreideweiss I, Ding Z, Galbarz L, Fu J, Jacoby C, Witzke O, Schrader J. Noninvasive detection of graft rejection by in vivo 19F MRI in the early stage. American Journal of Transplantation. 2011; 11: 235–244. [PubMed: 21214858]

81. Jacoby C, Borg N, Heusch P, Sauter M, Bönner F, Kandolf R, Klingel K, Schrader J, Flögel U. Visualization of immune cell infiltration in experimental viral myocarditis by 19F MRI in vivo. Magnetic Resonance Materials in Physics, Biology and Medicine. 2014; 27: 101–106.

82. Van Heeswijk RB, De Blois J, Kania G, Gonzales C, Blyszczuk P, Stuber M, Eriksson U, Schwitter J. Selective in vivo visualization of immune-cell infiltration in a mouse model of autoimmune myocarditis by fluorine-19 cardiac magnetic resonance. Circulation: Cardiovascular Imaging. 2013; 6: 277–284. [PubMed: 23343515]

83. Nahrendorf M, Sosnovik D, Chen JW, Panizzi P, Figueiredo J-L, Aikawa E, Libby P, Swirski FK, Weissleder R. Activatable Magnetic Resonance Imaging Agent Reports Myeloperoxidase Activity in Healing Infarcts and Noninvasively Detects the Antiinflammatory Effects of

Atorvastatin on Ischemia-Reperfusion Injury. Circulation. 2008; 117: 1153–1160. DOI: 10.1161/CIRCULATIONAHA.107.756510 [PubMed: 18268141]

84. Peterzan MA, Lewis AJM, Neubauer S, Rider OJ. Non-invasive investigation of myocardial energetics in cardiac disease using (31)P magnetic resonance spectroscopy. Cardiovasc Diagn Ther. 2020; 10: 625–635. DOI: 10.21037/cdt-20-275 [PubMed: 32695642]
85. Mahmod M, Pal N, Rayner J, Holloway C, Raman B, Dass S, Levelt E, Ariga R, Ferreira V, Banerjee R, et al. The interplay between metabolic alterations, diastolic strain rate and exercise capacity in mild heart failure with preserved ejection fraction: a cardiovascular magnetic resonance study. Journal of Cardiovascular Magnetic Resonance. 2018; 20: 88. doi: 10.1186/s12968-018-0511-6 [PubMed: 30580760]
86. Neubauer S. The failing heart--an engine out of fuel. N Engl J Med. 2007; 356: 1140–1151. DOI: 10.1056/NEJMra063052 [PubMed: 17360992]
87. Weiss RG, Bottomley PA, Hardy CJ, Gerstenblith G. Regional myocardial metabolism of high-energy phosphates during isometric exercise in patients with coronary artery disease. N Engl J Med. 1990; 323: 1593–1600. DOI: 10.1056/nejm199012063232304 [PubMed: 2233948]
88. Yabe T, Mitsunami K, Inubushi T, Kinoshita M. Quantitative measurements of cardiac phosphorus metabolites in coronary artery disease by 31P magnetic resonance spectroscopy. Circulation. 1995; 92: 15–23. DOI: 10.1161/01.cir.92.1.15 [PubMed: 7788910]
89. Bottomley PA, Weiss RG, Hardy CJ, Baumgartner WA. Myocardial high-energy phosphate metabolism and allograft rejection in patients with heart transplants. Radiology. 1991; 181: 67–75. DOI: 10.1148/radiology.181.1.1887057 [PubMed: 1887057]
90. Mahmod M, Francis JM, Pal N, Lewis A, Dass S, De Silva R, Petrou M, Sayeed R, Westaby S, Robson MD, et al. Myocardial perfusion and oxygenation are impaired during stress in severe aortic stenosis and correlate with impaired energetics and subclinical left ventricular dysfunction. J Cardiovasc Magn Reson. 2014; 16: 29. doi: 10.1186/1532-429x-16-29 [PubMed: 24779370]
91. Dass S, Cochlin LE, Suttie JJ, Holloway CJ, Rider OJ, Carden L, Tyler DJ, Karamitsos TD, Clarke K, Neubauer S, et al. Exacerbation of cardiac energetic impairment during exercise in hypertrophic cardiomyopathy: a potential mechanism for diastolic dysfunction. Eur Heart J. 2015; 36: 1547–1554. DOI: 10.1093/eurheartj/ehv120 [PubMed: 25990345]
92. Dass S, Holloway C, Suttie J, Mahmod M, Sever E, Watkins H, Neubauer S, Karamitsos T. Patients with Dilated Cardiomyopathy (DCM) have appropriate myocardial oxygenation response to vasodilator stress. Journal of Cardiovascular Magnetic Resonance. 2013; 15: O68. doi: 10.1186/1532-429X-15-S1-O68
93. Frieler RA, Mortensen RM. Immune cell and other noncardiomyocyte regulation of cardiac hypertrophy and remodeling. Circulation. 2015; 131: 1019–1030. DOI: 10.1161/CIRCULATIONAHA.114.008788 [PubMed: 25779542]
94. Friedrich J, Apstein CS, Ingwall JS. 31P nuclear magnetic resonance spectroscopic imaging of regions of remodeled myocardium in the infarcted rat heart. Circulation. 1995; 92: 3527–3538. DOI: 10.1161/01.cir.92.12.3527 [PubMed: 8521576]
95. Ardenkjaer-Larsen JH, Fridlund B, Gram A, Hansson G, Hansson L, Lerche MH, Servin R, Thaning M, Golman K. Increase in signal-to-noise ratio of > 10,000 times in liquid-state NMR. Proc Natl Acad Sci U S A. 2003; 100: 10158–10163. DOI: 10.1073/pnas.1733835100 [PubMed: 12930897]
96. Apps A, Lau J, Peterzan M, Neubauer S, Tyler D, Rider O. Hyperpolarised magnetic resonance for in vivo real-time metabolic imaging. Heart (British Cardiac Society). 2018; 104: 1484–1491. DOI: 10.1136/heartjnl-2017-312356 [PubMed: 29703741]
97. Almeida L, Lochner M, Berod L, Sparwasser T. Metabolic pathways in T cell activation and lineage differentiation. Semin Immunol. 2016; 28: 514–524. DOI: 10.1016/j.smim.2016.10.009 [PubMed: 27825556]
98. Pålsson-McDermott EM, O'Neill LAJ. Targeting immunometabolism as an anti-inflammatory strategy. Cell Res. 2020; 30: 300–314. DOI: 10.1038/s41422-020-0291-z [PubMed: 32132672]
99. Anderson S, Grist JT, Lewis A, Tyler DJ. Hyperpolarized (13) C magnetic resonance imaging for noninvasive assessment of tissue inflammation. NMR Biomed. 2021; 34 e4460-e4460 doi: 10.1002/nbm.4460 [PubMed: 33291188]

100. Apps A, Lau JYC, Miller JJJJ, Tyler A, Young LAJ, Lewis AJM, Barnes G, Trumper C, Neubauer S, Rider OJ, et al. Proof-of-Principle Demonstration of Direct Metabolic Imaging Following Myocardial Infarction Using Hyperpolarized 13C CMR. JACC Cardiovascular imaging. 2021; 14: 1285–1288. DOI: 10.1016/j.jcmg.2020.12.023 [PubMed: 33582059]

Europe PMC Funders Author Manuscripts

Summary

The immune system plays an integral role in many pathologies within the human heart. This may either be in response to an acute insult, such as ischemia or infectious agents, or due to more insidious pathologies in inflammatory cardiomyopathies, such as autoimmune myocarditis and sarcoidosis. Cardiovascular magnetic resonance (CMR), due to its superior ability to visualize myocardial tissue, has various techniques that enable non-invasive imaging of the immune system. Many methods are established and widely used, such as T2 weighted imaging, gadolinium-based contrast agents, and parametric mapping. These detect changes in the myocardial tissue that occur following immune system activation, such as edema, hyperemia and fibrosis (scar). Emerging methods focus on non-invasive imaging of the immune system directly, by imaging either the immune cells themselves through cell labelling or imaging their metabolic activity though magnetic resonance spectroscopy and hyperpolarized MRI. Further clinical trials are necessary to validate these methods prior to clinical adoption. If validated, the ability to image changes at cellular and molecular level could pave novel paths in our understanding of inflammatory cardiomyopathies, disease prognostication and personalized treatment regimes.

Europe PMC Funders Author Manuscripts

Europe PMC Funders Author Manuscripts

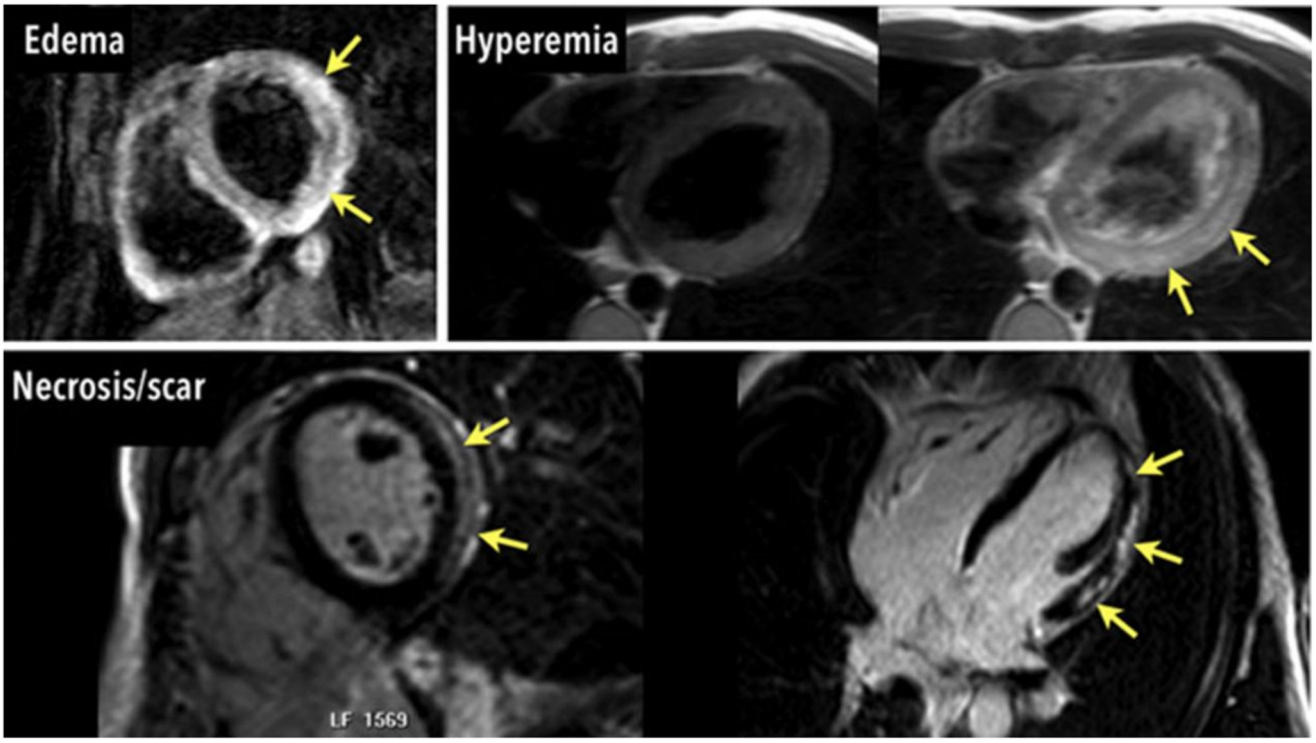

Figure 1.

Cardiovascular magnetic resonance criteria for myocarditis (Lake Louise Criteria) in the same patients: regional myocardial edema (**top left**), hyperemia in images acquired early after contrast injection (**top right**), and inflammatory necrosis in images acquired late (>10 minutes) after contrast injection (**bottom**). All 3 criteria are positive. As originally published by Wolters Kluwer Health, Inc in Friedrich and Marcotte, Circulation: Cardiovascular Imaging. 2013;6:834 [11]

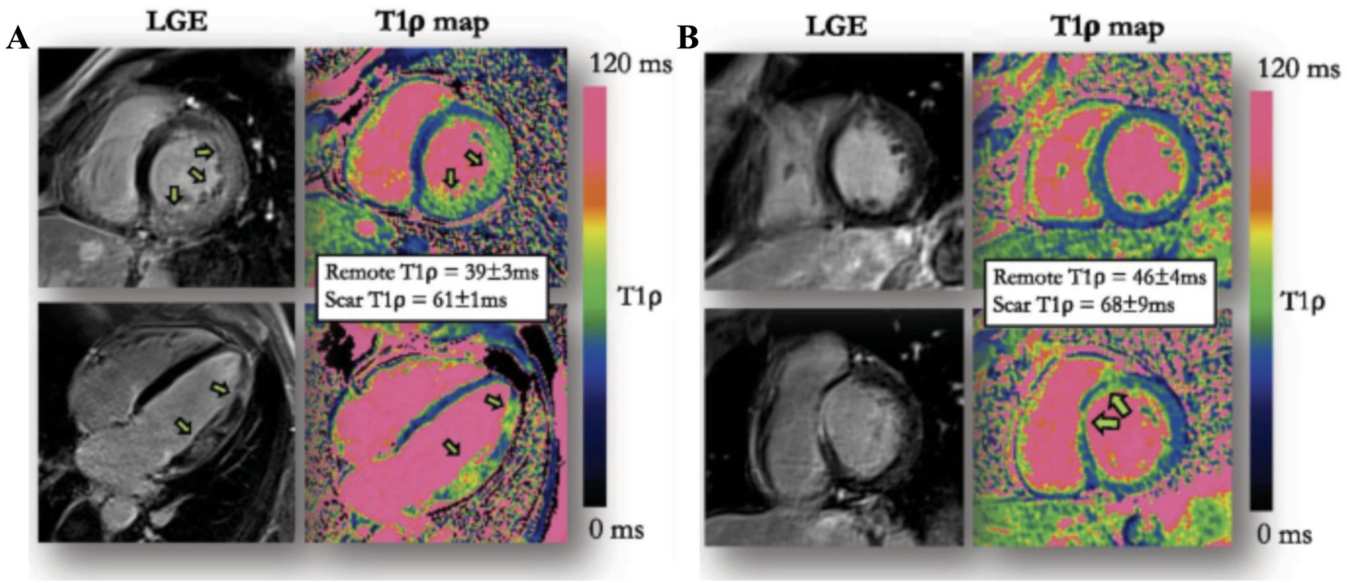

Figure 2.

A. 51-year-old male patient with acute myocarditis. Extensive patchy intramural and subepicardial late gadolinium enhancement (LGE) in the left ventricular free wall and the corresponding changes in T1rho-mapping. B. 35-year-old male patient with myocarditis. Intramural LGE in the basal antero-septal segment and the corresponding changes in T1rho-mapping. Modified image originally published by BMC in Bustin et al, J Cardiovasc Magn Reson. 2021;23(1):119[47].

Europe PMC Funders Author Manuscripts

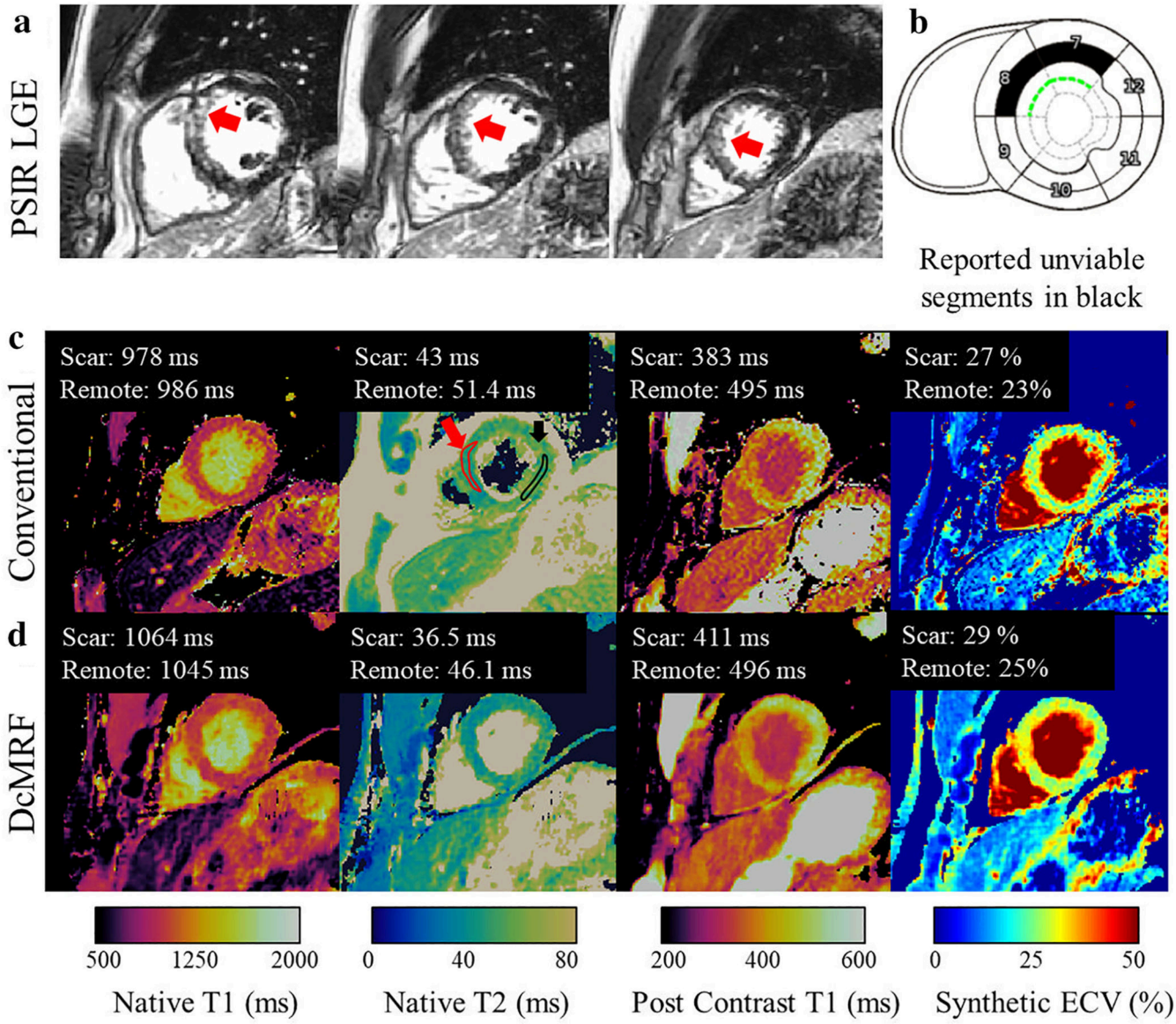

Figure 3. Patient with subendocardial chronic infarct.

(a) Phase-sensitive inversion recovery late gadolinium enhanced (PSIR LGE) images showing infarct (red arrow). (b) Diagram of reported unviable segments (c) conventional maps (d) cardiac MRF maps. Example ROIs drawn in the scar (red) and remote (black) areas are shown on the conventional T2 map (c). Water T1 (pre- and post-contrast), water T2, and synthetic ECV cardiac MRF values are in good agreement with conventional measurements. MRF = Magnetic Resonance Fingerprinting. ROI = Region of Interest. ECV = extracellular volume. As originally published by Wiley in Jaubert et al. Journal of Magnetic Resonance Imaging. 2021;53(4):1262[52]

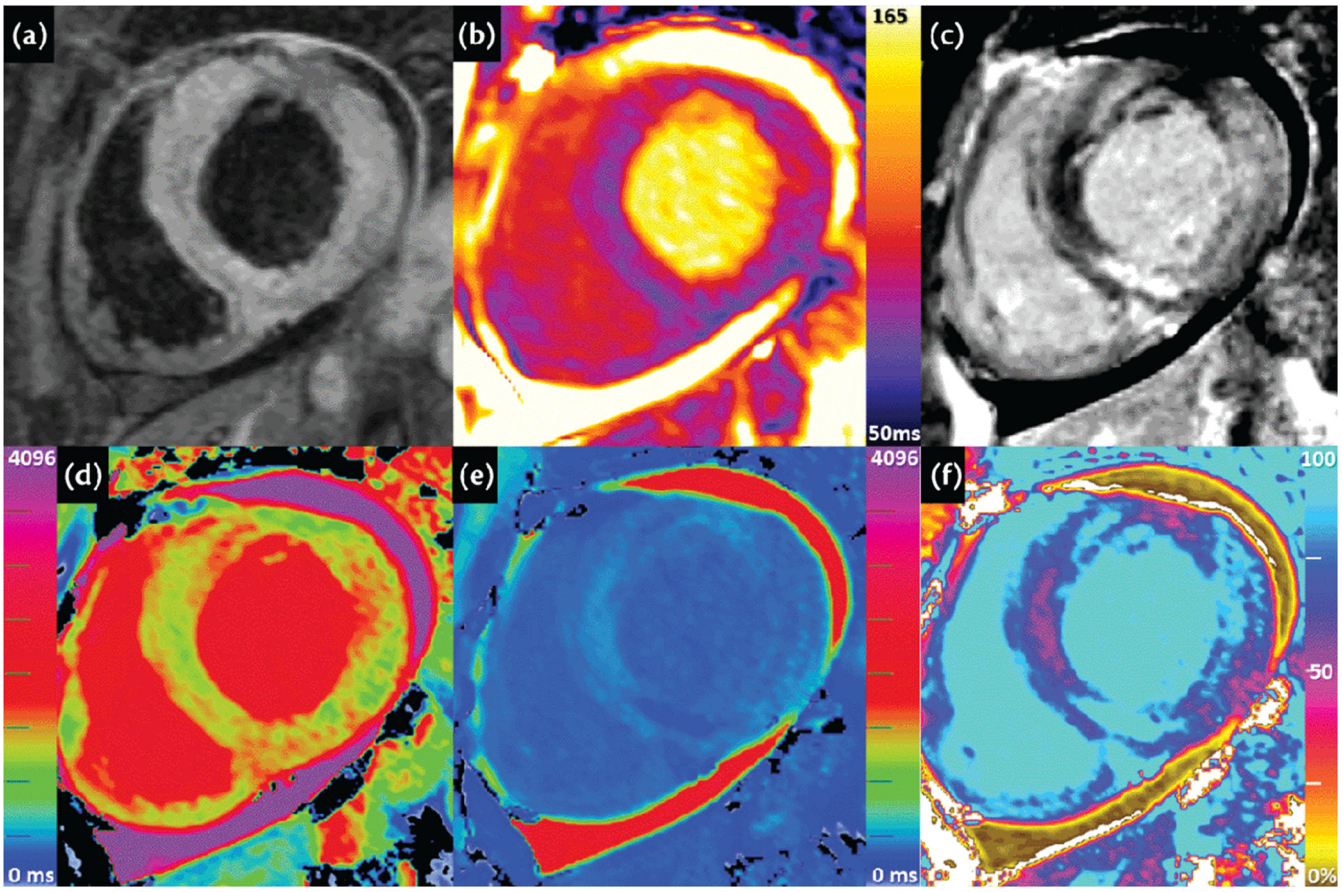

Figure 4. Cardiovascular magnetic resonance (CMR) images of a patient who presented with severe acute viral myocarditis.

(A) Dark-blood T2-weighted imaging showed global and focal increased myocardial T2 signal intensity, with a T2 signal intensity (SI) ratio compared to skeletal muscle (not shown) of > 3.0, consistent with severe acute edema. (B) T2-mapping showed global increase in myocardial T2 values of 89 ms (1.5 Tesla), consistent with edema. (C) Late gadolinium enhancement (LGE) imaging showed multiple areas of midwall, subepicardial and patchy enhancement in a non-coronary distribution. (D) Native T1-mapping using the ShMOLLI method showed significantly increased global myocardial T1 values (1048 ms; normal 962 ± 25 ms), and up to 1240 ms in focal areas of injury. (E) Post-gadolinium contrast T1-mapping (at 15 min) showed areas of very low T1 in areas of LGE. (F) Extracellular volume (ECV) mapping showed significantly expanded ECV of 43% (normal 27 ± 3 %). ShMOLLI = shortened modified Look-Locker inversion recovery. From: Ferreira VM et al. Myocarditis. In: The EACVI Textbook of Cardiovascular Magnetic Resonance M. Lombardi, V. Ferrari, C. Bucciarelli-Ducci, S. Petersen, and S. Plein, Eds. Oxford, UK: Oxford University Press 2018. [55]

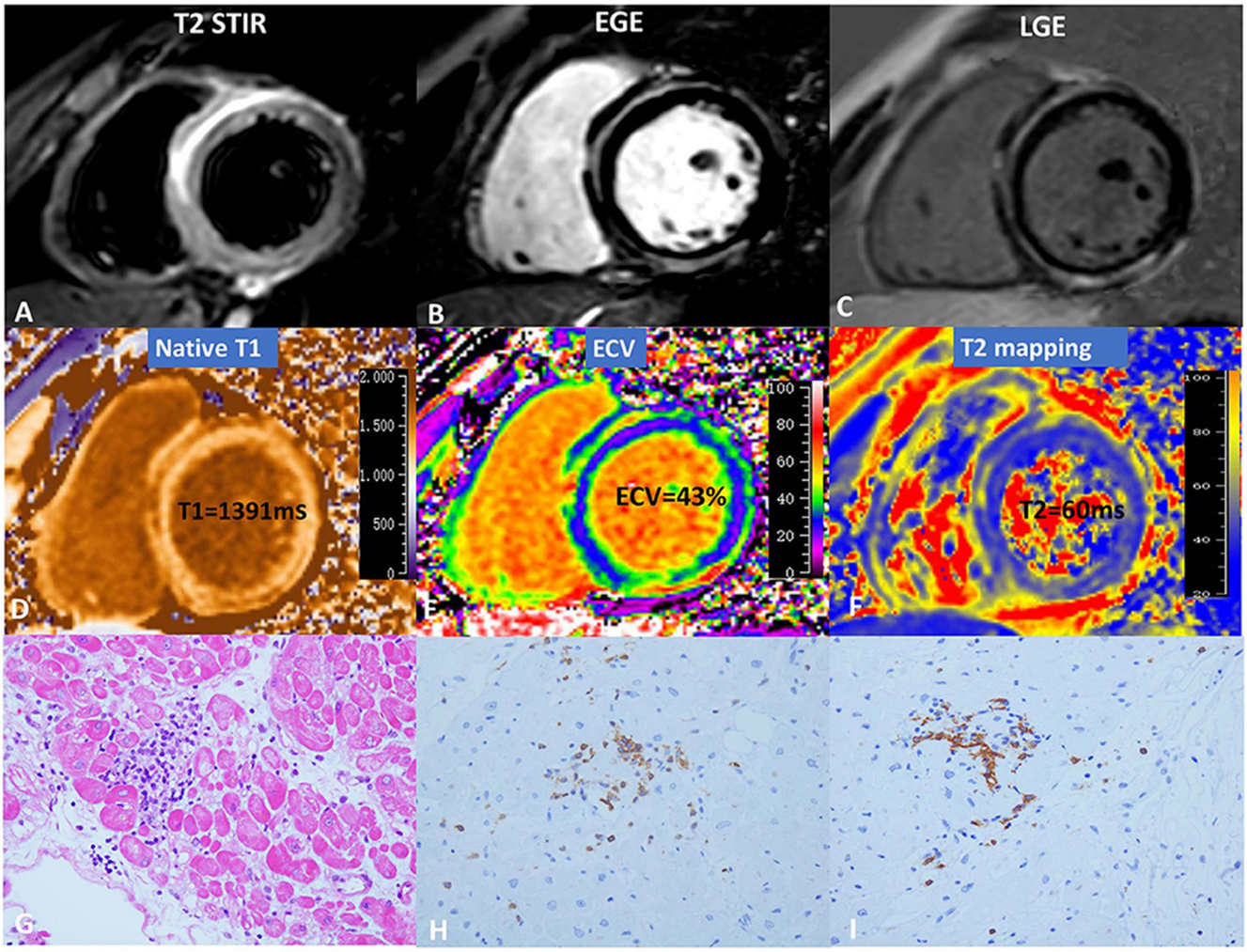

Figure 5. Cardiovascular magnetic resonance (CMR) and pathology results for a representative case of myocarditis.

(A) T2-STIR, (B) EGE, (C) LGE, (D) native T1, (E) ECV, and (F) T2-mapping. (G) indicates focal myocyte damage with lymphocytic infiltration. Immunohistochemistry revealed (H) LCA + (x40) and (I) CD20 + (x40). As originally published by Open Access Frontiers in Li et al. Frontiers in Cardiovascular Medicine. 2021;8:739892. T2 STIR = T2 short-tau inversion recovery, EGE = early gadolinium enhancement, LGE = late gadolinium enhancement, ECV = extracellular volume, LCA = leukocyte common antigen, CD = cluster of differentiation [70]

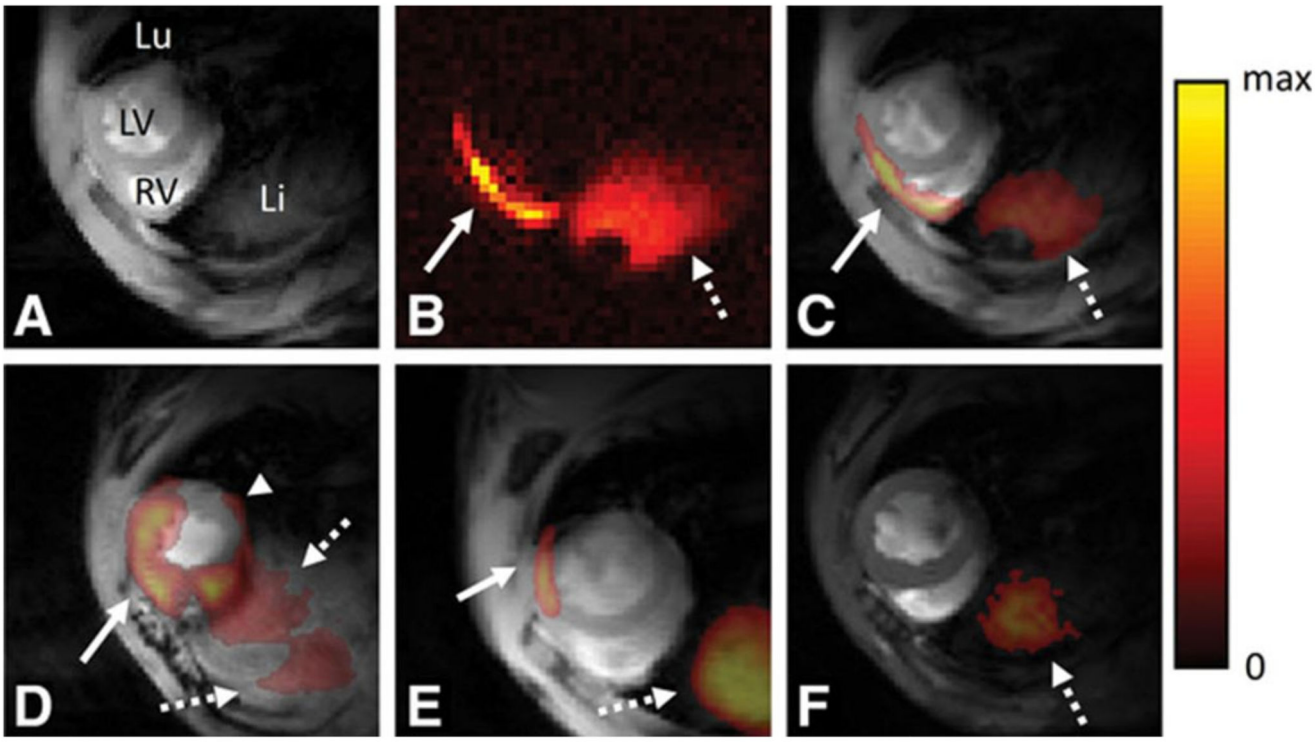

Figure 6. In vivo fluorine-19 (^{19}F)-cardiovascular magnetic resonance (CMR) of myocarditis.

A, ^{1}H CMR slice in the short-axis orientation at the base of the heart of a mouse with disease score 3; ^{1}H CMR depicts the right and left ventricles (RV and LV) as well as the lung (Lu) and liver (Li). **B**, ^{19}F-CMR of the same anatomic location. Two regions with a ^{19}F signal can be observed: a thin line at the level of the myocardium (solid **arrow**) and a larger region at the level of the liver (dotted **arrow**). The color coding for ^{19}F signal intensity is given to the right (in arbitrary units). **C**, Fusion of the ^{1}H (**A**) and ^{19}F images (**B**): the ^{19}F signal colocalizes with the subepicardial layer of the LV anterior wall, the RV free wall (**arrow**) and the liver (dotted **arrow**). **D**, A similar fused basal slice in an animal with disease score 4. Here, the ^{19}F signal is spread over the majority of the ventricles with a subepicardial ^{19}F signal in the inferior wall of the LV (**arrow head**). **E**, Animal with disease score 2 with a relatively small patch of ^{19}F signal (**arrow**). **F**, Healthy control, in which a ^{19}F signal can only be observed in the liver (dotted **arrow**). As originally published by Wolters Kluwer Health, Inc in van Heeswijk et al. Circ Cardiovasc Imaging. 2013;6(2):280 82

Europe PMC Funders Author Manuscripts

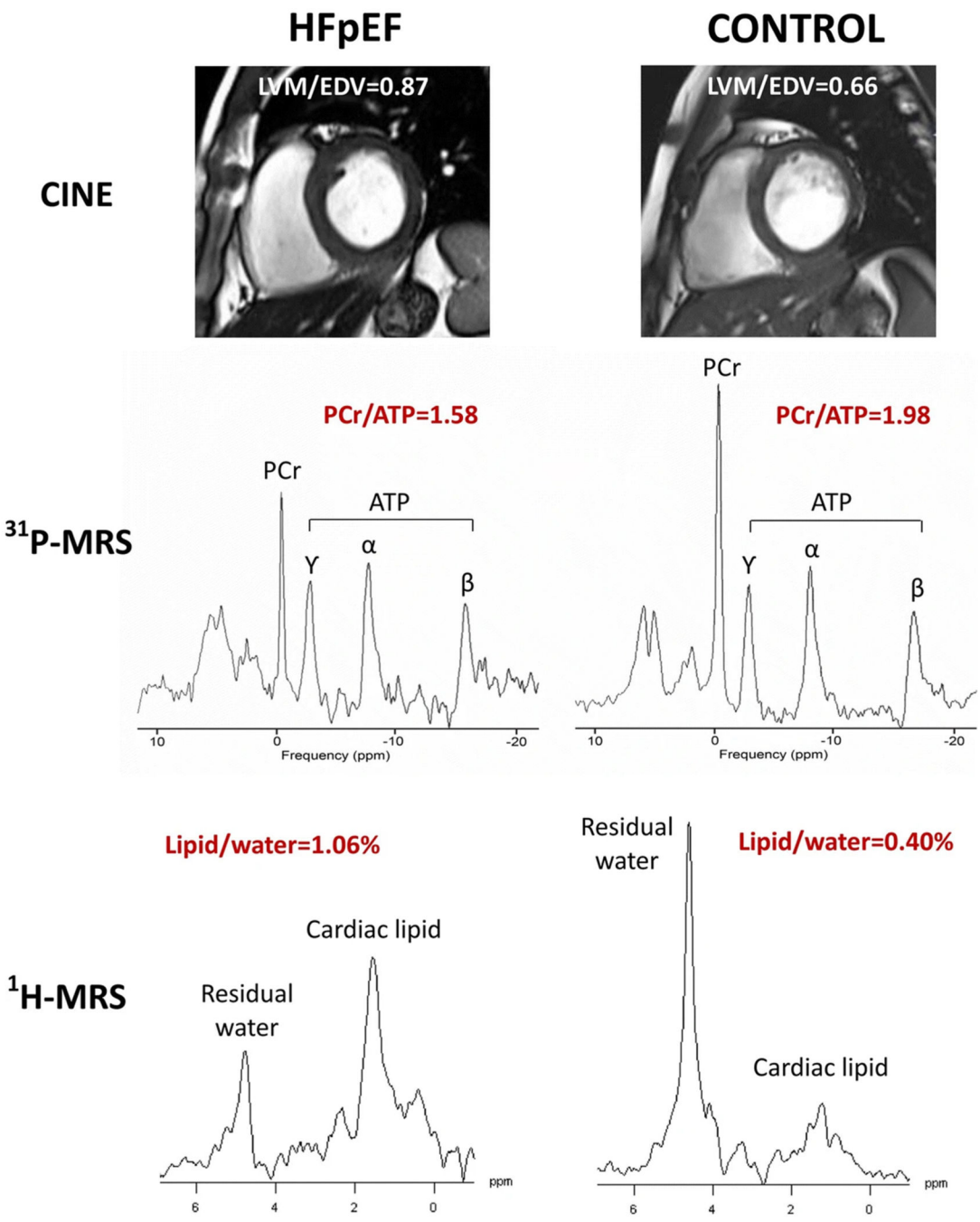

Figure 7.

Representative results of LVM/EDV, PCr/ATP and Lipid/water for heart failure with preserved ejection fraction (HFpEF) (left) and control (right). Cine imaging (top panel), ^{31}P-CMRS (middle panel) and ^{1}H-CMRS (bottom panel). ^{1}H-CMRS spectra are scaled based on unsuppressed water (not shown) and noise level. LVM = left ventricular mass; EDV = end-diastolic volume; PCr = phosphocreatine; ATP = adenosine triphosphate; CMRS = cardiovascular magnetic resonance spectroscopy. As originally published by Springer Nature in Mahmod et al. Journal of Cardiovascular Magnetic Resonance. 2018;20(1):88 [85]

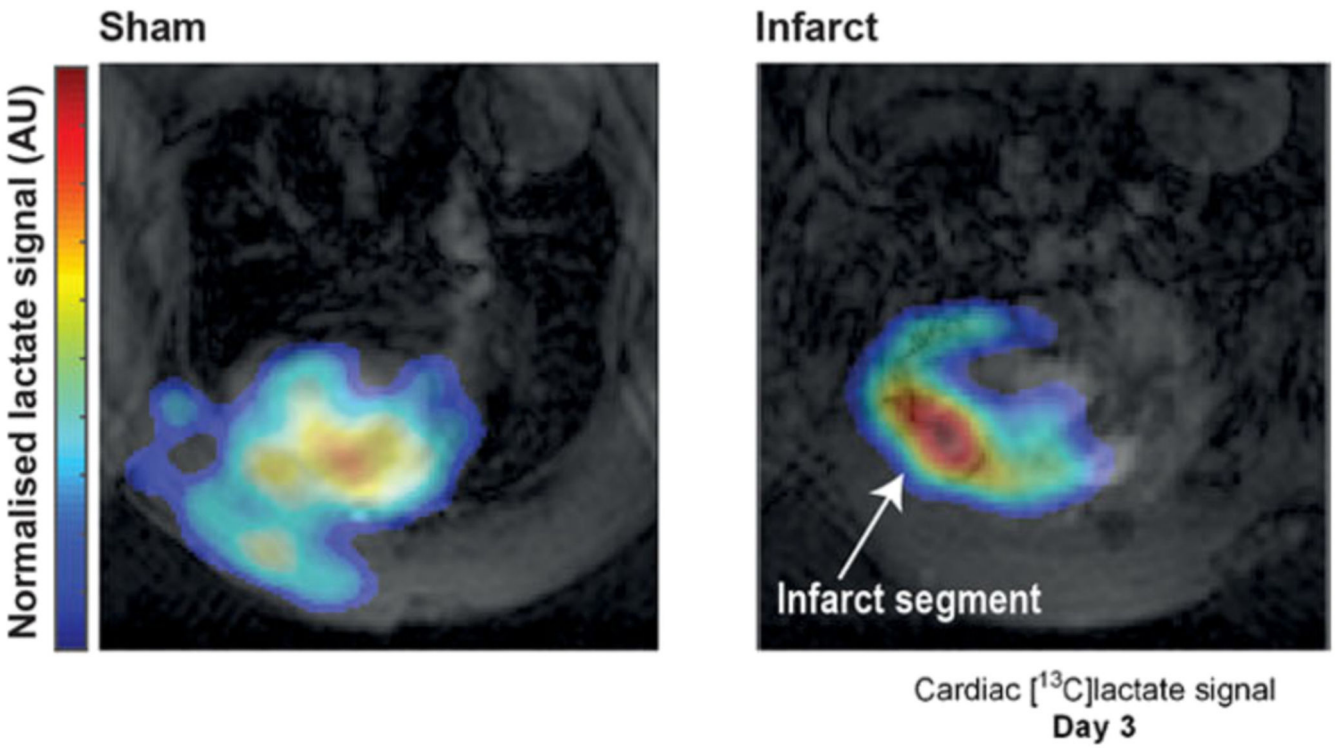

Figure 8.

Hyperpolarized [13C]lactate generation in a rodent model of cryoinfarction at 3 days post-experimental myocardial infarction compared to sham. Modified image originally published by Wiley in Anderson et al. NMR in Biomedicine. 2021;34(3):e4460 [99]

Europe PMC Funders Author Manuscripts

Europe PMC Funders Author Manuscripts

Table 1

A summary of the original (2009)[39] and revised (2018)[12] Lake Louise criteria

Lake Louise criteria
Lake Louise Criteria (2009)[39]:
In the setting of clinically suspected myocarditis, CMR findings are consistent with myocardial inflammation if at least 2 of the following 3 criteria are present:
- Regional or global myocardial SI increase in T2-weighted images (edema)
- Increased global myocardial early gadolinium enhancement ratio between myocardium and skeletal muscle in gadolinium-enhanced T1-weighted images (hyperemia)
- At least 1 focal lesion with nonischemic regional distribution in inversion recovery-prepared gadolinium-enhanced T1-weighted images (*LGE*) (necrosis/fibrosis)
The presence of LV dysfunction or pericardial effusion provides additional, supportive evidence or myocarditis.
Updated Lake Louise criteria (2018)[12]:
Any 2 out of 2 are present:
- T2-based imaging: regional high T2 SI *or* Global T2 SI ratio ≥ 2.0 in T2W CMR images *or* Regional or global increase of myocardial T2 relaxation time
- T1-based imaging: regional or global increase of native myocardial T1 or ECV *or* areas with high SI in a nonischemic distribution pattern in LGE images
Supportive criteria:
- Pericardial effusion in cine CMR images *or* High signal intensity of the pericardium in LGE images, T1-mapping or T2-mapping
- Systolic LV wall motion abnormality in cine CMR images

CMR = cardiac magnetic resonance LGE = late gadolinium enhancement LV = left ventricle

SI = signal intensity T2W = T2-weighted ECV = extracellular volume